A. ANMA, K. SAKAMOTO AND T. YONEDA
KODAI MATH. J.
35 (2012), 215–247

UNSTABLE SUBSYSTEMS CAUSE TURING INSTABILITY

Atsushi Anma, Kunimochi Sakamoto and Tohru Yoneda

Abstract

We study Turing instabilities in 3-component reaction-diffusion systems. The existence of a *complementary pair* of stable-unstable subsystems always gives rise to Turing instability for suitable diagonal diffusion matrices. There are two types of Turing instability, one called *steady instability* and the other *wave instability*. To determine which of the two types of instability actually occurs, easily verifiable conditions on unstable subsystems are given. A complementary pair of *unstable-unstable* subsystems in a stable full system also leads to steady instability. Our results give a perspective to the rich variety and complexity of pattern dynamics in 3-component systems of reaction-diffusion equations at the onset.

1. Background, problem and main result

In 1952, Turing [16] proposed a novel idea that two chemical substances reacting and diffusing in a homogeneous medium might produce a stable spatially inhomogeneous state, out of a uniform steady state which is stable under homogeneous perturbations. This statement sounds counter intuitive, because diffusion supposedly acts as a stabilizing (homogenizing) effect. Turing, however, clearly demonstrated, via a concrete system of two linear reaction-diffusion equations, that this (mathematical) phenomenon certainly is possible. Despite of (*or "Because of"*) its counter intuitive nature, this fascinating idea has attracted the attention of researchers from diverse areas of science, such as biology, nonlinear physics, chemistry, engineering, as well as mathematics, and a huge amount of literature on this subject has accumulated, see for example [1, 4, 6, 10] and references there.

Most studies on Turing instability have been concerned with 2-component systems of reaction-diffusion equations, and the mathematical mechanism of Turing instability is well-understood for 2-component systems [1, 4, 6, 10]. In the original article [16], however, Turing also touched on 3-component systems and briefly mentioned to a type of instability associated with a mode which is nontrivial both in *space* and *time*, as quoted below:

> §8.7. *Oscillatory case with a finite wave length* (*case e*). *This means that there are genuine travelling waves. Since the example to be given*

Received August 18, 2011; revised January 5, 2012.

involves three morphogens it is not possible to use the formulae of Section 6. Instead, one must use the corresponding three morphogen formulae.

This type of Turing instability never occurs in 2-component systems, as long as the diffusion matrix is diagonal.

In recent decades, there have been several papers [13, 19, 18, 12, 7] dealing with Turing instability in 3-component systems of reaction-diffusion equations, and each of these investigations extends the Turing instability mechanism to 3-component systems. To our best knowledge, however, there is no comprehensive mathematical description of what the essential feature of Turing instability is in n-component $(n \geq 3)$ systems.

The purpose of this article is to clarify the source of Turing instabilities and how they appear in 3-component systems of reaction-diffusion equations.

In the remaining part of §1, we formulate our problem in precise terms, present main results and relate our results to other previous studies. Proofs of the main results are given in §2. We apply the main results to several concrete examples in §3. Finally, in §4, we display types of stable 3×3 matrices in which various stability-instability properties of sub-matrices coexist, and give a perspective for remaining problems.

1.1. Statement of problem. We consider the 3-component system of reaction-diffusion equations;

$$\frac{\partial u}{\partial t} = d_1 \triangle u + F(u, v, w), \quad \frac{\partial v}{\partial t} = d_2 \triangle v + G(u, v, w), \tag{1.1}$$
$$\frac{\partial w}{\partial t} = d_3 \triangle w + H(u, v, w),$$

where $\triangle$ stands for the Laplace operator and $d_j \geq 0$ $(j = 1, 2, 3)$ are diffusion coefficients of the components u, v, w, respectively. We assume that the nonlinear reaction terms F, G, H are smooth. Throughout this article, the spatial domain and boundary conditions associated with (1.1) are not specified. Instead, we only use the eigenvalues $-\mu \leq 0$ of the Laplace operator $\triangle$ in various domains under suitable (presumably, no flux or periodic) boundary conditions. This is sufficient for the purpose of this article.

Suppose that (1.1) has a homogeneous steady state $(u, v, w) = (u_0, v_0, w_0)$ which is stable under homogeneous perturbation, i.e., $(u, v, w) = (u_0, v_0, w_0)$ is an asymptotically stable steady state with respect to the system of ordinary differential equations

$$\frac{\mathrm{d}u}{\mathrm{d}t} = F(u, v, w), \quad \frac{\mathrm{d}v}{\mathrm{d}t} = G(u, v, w), \quad \frac{\mathrm{d}w}{\mathrm{d}t} = H(u, v, w), \tag{1.2}$$

which is obtained from (1.1) by dropping the diffusion terms. Our main concern here is the linearized version of (1.1);

$$\frac{\partial}{\partial t} U = D \triangle U + AU, \tag{1.3}$$

where $U = (u, v, w)$, $D = \mathrm{diag}(d_1, d_2, d_3)$ is the 3×3 diffusion matrix, and A is the linearization of the vector field (F, G, H) at (u_0, v_0, w_0).

Detecting the Turing instability of the homogeneous state (u_0, v_0, w_0) amounts to finding a suitable diffusion matrix D for which (1.3) has exponentially growing solutions. Since (1.3) is homogeneous both in space and time, its solutions are easily found to be of the form

$$U(t, x) = \mathrm{e}^{\lambda(\mu)t}\Phi_\mu(x),$$

or linear combinations of such solutions, where the *growth exponents* $\lambda(\mu)$ are the eigenvalues of the 3×3 matrix $-\mu D + A$, and Φ_μ are the product of the eigenfunctions of the Laplace operator $\triangle$ associated with the eigenvalue $-\mu$ and the eigenvectors of $-\mu D + A$. (To be precise, the eigenvalues $\lambda(\mu)$ also depend on D and A. They are sometimes expressed as $\lambda(\mu, D)$ or $\lambda(\mu, D, A)$, according to our needs.) Therefore, to find an exponentially growing solution of (1.3), it is necessary and sufficient to find D and $\mu \geq 0$ for which $\mathrm{Re}\, \lambda(\mu, D) \geq 0$ is realized. On the other hand, the assumption that $(u, v, w) = (u_0, v_0, w_0)$ is asymptotically stable relative to the dynamics of (1.2) implies that the eigenvalues of A have negative real part. Therefore, our problem is formulated as follows.

Problem: For a stable 3×3 matrix A, find a diagonal diffusion matrix D for which there exists an eigenvalue $\mu > 0$ of the Laplace operator $\triangle$ satisfying $\mathrm{Re}\, \lambda(\mu, D, A) \geq 0$.

Throughout this article, a square matrix A of any size is called *stable* if all eigenvalues of A have negative real part, and A is called *unstable* if it is not stable.

1.2. Turing-instability for 3-component systems. For a 3×3 matrix $A = (a_{jk})$, 1- and 2-component subsystems A_j $(j = 1, 2, 3)$ and A_{jk} $(1 \leq j, k \leq 3, j \neq k)$, respectively, are defined as follows: $A_j = a_{jj}$, $(j = 1, 2, 3)$ and A_{jk} is the 2×2 submatrix obtained from A by taking exactly the rows and the columns of indices j, k. A pair (A_m, A_{jk}) is said to form a *complementary pair* in A, if $\{m, j, k\} = \{1, 2, 3\}$. There are three complementary pairs (A_1, A_{23}), (A_2, A_{13}), (A_3, A_{12}).

Although the main results of this article contain several sub-cases, they are summarized as Main Feature below. Before stating it, we give the precise definition of Turing instability for the purpose of this article.

Definition 1.1. Let A be a stable 3×3 matrix and D a 3×3 diagonal diffusion matrix. We denote by $\lambda(\mu, D)$ the eigenvalues of $-\mu D + A$.

(i) If one eigenvalue $\lambda(\mu, D)$ crosses 0 from negative to positive along the real axis in the complex plane for some $\mu > 0$ as D varies, then we say that *steady instability* (*S-instability*, for short) occurs for (1.3). If, moreover, the remaining eigenvalues of $-\mu D + A$, for all $\mu > 0$ and for such D that $\lambda(\mu, D) = 0$, stay in the left half complex plane, then we say that the steady instability is *primary* (*primary S-instability*, for short). In these situations, the quantity $\kappa_S = \sqrt{\mu}$ is called the *S-wave number*.

(ii) If a non-real eigenvalue $\lambda(\mu, D)$ and its complex conjugate cross the imaginary axis from the left half plane to the right half plane for some $\mu > 0$ as D varies, then we say that *wave instability* (*W-instability*, for short) occurs for (1.3). If, moreover, the remaining eigenvalues of $-\mu D + A$, for all $\mu > 0$ and for D such that $\operatorname{Re}\lambda(\mu, D) = 0$, stay in the left half complex plane, then we say that the wave instability is *primary* (*primary W-instability*, for short). In these situations, the quantity $\kappa_W = \sqrt{\mu}$ is called the *W-wave number*.

These two types of instability are called *Turing instability*.

Note that W-instability is impossible for 2-component systems if the diffusion matrix D is diagonal. With this definition, the main feature of our results for 3-component systems is summarized as follows.

Main Feature. *Suppose that the* 3×3 *matrix* A *is stable and* (A_m, A_{jk}) *forms a complementary pair in* A.

(i) *If* A_{jk} *is unstable, then a Turing instability occurs for diffusion matrices* D *that satisfy* $d_m \gg \max\{d_j, d_k\}$.

(ii) *If* $A_m > 0$ *is unstable, then a Turing instability occurs for diffusion matrices* D *that satisfy* $\min\{d_j, d_k\} \gg d_m$.

In other words,

> *if the diffusion rate of an unstable subsystem in a stable full system is sufficiently small compared with the diffusion rate of its complementary partner, then a diffusion-induced instability readily sets in.*

The Turing instability mechanism in 2-component systems naturally conforms to the statements of Main Feature. It is well known [1, 4, 6, 10] that for a stable 2×2 matrix B, Turing instability occurs only if B is one of the following types;

$$B = \begin{pmatrix} + & - \\ + & - \end{pmatrix}, \quad B = \begin{pmatrix} - & + \\ - & + \end{pmatrix}, \quad B = \begin{pmatrix} - & - \\ + & + \end{pmatrix}, \quad B = \begin{pmatrix} + & + \\ - & - \end{pmatrix}.$$

Among these four types, the first and the second (respectively, the third and the fourth) are essentially the same. Each one of these 2×2 matrices consists of a complementary pair of stable-unstable subsystems, and the fact that their off-diagonal entries are of opposite sign is forced from the stability requirements of the full 2×2 system B. Moreover, the diffusion induced instability actually occurs when the diffusion rate of unstable component is sufficiently small relative to the diffusion rate of the stable component. We may well say that Main Feature extends the Turing instability mechanism to a 3-component version.

In order to make Main Feature a little more useful in practice, its statements must be made more precise. For the purpose, we classify the instability of a 2-component subsystem A_{jk} into three types by negating its stability conditions $\operatorname{tr} A_{jk} < 0$ and $\det A_{jk} > 0$. We only consider *semi-generic situations*.

Definition 1.2. Let A_{jk} be a 2-component subsystem of A. It is called
(1) *type-1 unstable*, if $\operatorname{tr} A_{jk} > 0$ and $\det A_{jk} \geq 0$,
(2) *type-2 unstable*, if $\operatorname{tr} A_{jk} \leq 0$ and $\det A_{jk} < 0$,
(3) *type-3 unstable*, if $\operatorname{tr} A_{jk} > 0$ and $\det A_{jk} < 0$.

We are now ready to state our main results.

Theorem 1.1. *Suppose that A is a stable 3×3 matrix and the pair (A_m, A_{jk}) forms a complementary pair in A.*

(i) *If $A_m > 0$ is unstable and A_{jk} is stable, then for any $d_j > 0$, $d_k > 0$, S-instability occurs for diffusion matrices D that satisfy $d_m \ll \min\{d_j, d_k\}$.*
(ii) *If A_{jk} is type-1 unstable and A_m is stable, then for any $d_m > 0$, W-instability occurs for diffusion matrices D that satisfy $\max\{d_j, d_k\} \ll d_m$.*
(iii) *If A_{jk} is type-2 unstable and A_m is stable, then for any $d_m > 0$, S-instability occurs for diffusion matrices D that satisfy $\max\{d_j, d_k\} \ll d_m$.*
(iv) *If A_{jk} is type-3 unstable and A_m is stable, then for any $d_m > 0$, both S-instability and W-instability occur for diffusion matrices D that satisfy $\max\{d_j, d_k\} \ll d_m$.*
(v) *If $A_m > 0$ is unstable and A_{jk} is type-2 unstable, then*
   (a) *for any $d_m > 0$, S-instability occurs for diffusion matrices D that satisfy $\max\{d_j, d_k\} \ll d_m$;*
   (b) *for any $d_j > 0$, $d_k > 0$, S-instability occurs for diffusion matrices D that satisfy $\min\{d_j, d_k\} \gg d_m$.*

Concerning the statements of this theorem, several remarks are to be made.

- We notice that S-instability is associated with a 1-component unstable subsystem and a type-2 unstable subsystem. On the other hand, W-instability occurs when a type-1 unstable or type-3 unstable subsystem is involved in a complementary pair.
- In Theorem 1.1 above, we do *not* claim that the S- or W-instability must be *primary*. This indefiniteness is due to the fact that there may be more than one complementary pairs consisting of at least one unstable subsystem in a stable full system, and that the Turing instability mechanisms originating from the different complementary pairs may interact.
- If two complementary pairs other than the pair (A_m, A_{jk}) in Theorem 1.1 (i) are of stable-stable type, then the S-instability is primary (cf. Corollary 1.1 (i), below).
- If 2-component subsystems other than A_{jk} in Theorem 1.1 (iii) are stable, then the S-instability is primary (cf. Corollary 1.1 (ii), below).
- In Theorem 1.1 (ii), W-instability is primary for suitable diffusion matrices with $\max\{d_j, d_k\} \ll d_m$ (cf. Corollary 1.1 (iii) and (iv), below).
- In Theorem 1.1 (iv), the S- and W-instability mechanisms may interact within a type-3 unstable subsystem. If S- and W-instability occur for the

same diffusion rates, the corresponding wave numbers tend to behave as follows:

$$\text{If } \operatorname{tr} A_{jk} \ll |\det A_{jk}|, \quad \text{then } \kappa_{\mathrm{W}} \gg \kappa_{\mathrm{S}}.$$

$$\text{If } \operatorname{tr} A_{jk} \gg |\det A_{jk}|, \quad \text{then } \kappa_{\mathrm{W}} \ll \kappa_{\mathrm{S}}.$$

However, in case $\operatorname{tr} A_{jk} \ll |\det A_{jk}|$, S-instability seems to be always primary and W-instability is hardly observable. On the other hand, in case $\operatorname{tr} A_{jk} \gg |\det A_{jk}|$ both S- and W-instability may occur for the same diffusion matrix D ([8, 18, 19]), and it has been reckoned that $\kappa_{\mathrm{W}} < \kappa_{\mathrm{S}}$ is a rule. We will show in §3 that this rule is violated by an example.

- Concerning statement (v) of Theorem 1.1, one may wonder if an unstable-unstable complementary pair comprises a stable matrix A. This is, of course, impossible in 2-component systems. However, in 3-component systems, this is true for an open set of matrices (cf. examples in §3). In this situation, the subsystem A_{jk} must necessarily be type-2 unstable.

There are situations in which Turing instabilities do not occur. Results in this direction are summarized as follows.

Theorem 1.2. *Suppose that A is a stable 3×3 matrix.*

(i) *If all 1-component and 2-component subsystems are stable, then Turing instability never occurs for any choice of the diffusion matrix D.*

(ii) *If all 2-component subsystems are stable, then W-instability never occurs for any choice of the diffusion matrix D.*

(iii) *If A_{jk} is type-2 unstable and its complementary A_m is stable, then W-instability does not occur for diffusion matrices D that satisfy $\max\{d_j, d_k\} \ll d_m$. If, moreover, 2-component subsystems other than A_{jk} are stable, then W-instability does not occur for diffusion matrices D that satisfy $\max\{d_j, d_k\} \le d_m$.*

(iv) *Suppose that A_m is stable and its complementary A_{jk} is type-1 unstable with $A_j > 0 > A_k$. If either*
(1) $\det A_{jm} < 0$ *and* $\det A_{km} < 0$, *or*
(2) $\det A_{km} \ge 0$,
then S-instability does not occur for diffusion matrices D that satisfy $\max\{d_j, d_k\} \le d_m$ and $d_k \le (-A_k/A_j) d_j$.

(v) *Suppose that A_m is stable and its complementary A_{jk} is type-1 unstable with $A_j > 0$ and $A_k > 0$. If either*
(1) $\det A_{jm} \ge 0$, $\det A_{km} \ge 0$ *and* $\det A_{jk} > A_j A_k$, *or*
(2) $\det A_{jm} < 0$, $\det A_{km} < 0$ *and* $p_2 > A_j A_k$,
then there exist ℓ_1, ℓ_2 with $0 < \ell_1 < (A_k/A_j) < \ell_2$ so that S-instability does not occur for diffusion matrices D that satisfy $\max\{d_j, d_k\} \le d_m$ and $\ell_1 d_j \le d_k \le \ell_2 d_j$.

Combining Theorems 1.1 and 1.2, we immediately obtain several sufficient conditions for *primary* Turing instabilities.

COROLLARY 1.1. *Suppose that A is a stable 3×3 matrix.*

(i) *If $A_m > 0$ is an unstable subsystem and all 2-component subsystems are stable, then for any $d_j > 0$, $d_k > 0$, S-instability* primarily *occurs for diffusion matrices D that satisfy $d_m \ll \min\{d_j, d_k\}$.*

(ii) *If a type-2 unstable A_{jk} and a stable A_m form a complementary pair in A, and if 2-component subsystems other than A_{jk} are stable, then for any $d_m > 0$, S-instability* primarily *occurs for diffusion matrices D that satisfy $\max\{d_j, d_k\} \ll d_m$.*

(iii) *If A_m is stable and its complementary A_{jk} is type-1 unstable with $A_j > 0 > A_k$, and if either*

(1) $\det A_{jm} < 0$ *and* $\det A_{km} < 0$, *or*

(2) $\det A_{km} \geq 0$,

then W-instability primarily *occurs for diffusion matrices D that satisfy $\max\{d_j, d_k\} \ll d_m$ and $d_k < (-A_k/A_j)d_j$.*

(iv) *If A_m is stable and its complementary A_{jk} is type-1 unstable with $A_j > 0$ and $A_k > 0$, and if either*

(1) $\det A_{jm} \geq 0$, $\det A_{km} \geq 0$ *and* $\det A_{jk} > A_j A_k$, *or*

(2) $\det A_{jm} < 0$, $\det A_{km} < 0$ *and* $p_2 > A_j A_k$,

then there exist ℓ_1, ℓ_2 with $0 < \ell_1 < (A_k/A_j) < \ell_2$ so that W-instability primarily *occurs for diffusion matrices D that satisfy $\max\{d_j, d_k\} \ll d_m$ and $\ell_1 d_j \leq d_k \leq \ell_2 d_j$.*

There are many previous studies on *necessary* and/or *sufficient* conditions for Turing instability in n-component ($n \geq 3$) systems of reaction diffusion equations. We only mention to some representatives of such studies which caught our attention.

Othmer and Scriven in [9] considered reaction equations with general diffusion matrices with *cross-diffusion* effects, and studied various possibilities of Turing-type instability, by closely examining the behavior of the eigenvalues $\lambda(\mu)$ of the matrix $-\mu D + A$ for $\mu \geq 0$. In [15], a *cross-inhibition* effect in A (i.e., $a_{ij} < 0$ for some $i \neq j$) was identified as a necessary condition for Turing instability. In [11, 12], it was shown that if all possible subsystems are stable then Turing instability never occurs (hence, our Theorem 1.2 (i) is not new), although the main interest of [11, 12] was in another destabilization mechanism called *differential flow induced instability*. For mass-action type reaction equations, a graph theoretic method was applied in [5] to characterize, as a necessary condition for Turing instability, a so called *critical fragment condition* which is equivalent to the existence of an auto-catalytic subsystem (unstable subsystem). For a concrete system of reaction diffusion-equations describing the dynamics among three species (host-parasite-hyperparasite), [18] developed a theoretical framework, similar to that of this article, for Turing instabilities and displayed the occasions where S- and W-instabilities are actually induced. The importance of stable-unstable complementary pairs for Turing instability seems to have been envisaged in [13], although the idea was neither thoroughly scrutinized nor fully developed. The authors of [13] claimed that the necessary and sufficient conditions for the Turing instability were established by Theorems 1 and 3 in [13]. However, Theorem 3 in [13] (sufficiency for Turing instability) is not complete in the sense that it does not take care of the possibility of W-instability, and [13] is amended by [14] which contains an example of a 4-component system indicating the possibility of W-instability. In [19], 3-component systems (the extended Brusselator model and the extended Oregonator model) were numerically studied to exhibit a variety of spatiotemporal patterns arising from the interaction of the stationary Turing and oscillatory Turing instabilities. The authors of [7] experimentally identified the interaction network between the pigment cells of zebrafish, and showed, by using a 3-component system of reaction-diffusion equations, that this interaction network possesses the properties necessary to induce Turing patterns, in which two variables representing the density of the 2 types of pigment cells, *melanophores* and *xanthophores*, form a 2-component unstable subsystem.

As far as 3-component systems are concerned, the generality and variety of the onset of instability in the above-mentioned results are altogether covered by our results in Theorems 1.1, 1.2 and Corollary 1.1, except for cross diffusion effects.

2. Proof of main results

Once the statements are properly made, the results in §1 are proved by using the Routh-Hurwitz criterion [3] in an elementary manner. Let $P(\lambda) = \lambda^3 + p_1\lambda^2 + p_2\lambda + p_3$ be the characteristic polynomial of the 3×3 matrix A. The coefficients p_j $(j = 1, 2, 3)$ are given by

$$p_1 = -\mathrm{tr}\, A, \quad p_2 = \det A_{12} + \det A_{23} + \det A_{13}, \quad p_3 = -\det A.$$

Here and below, we use sub-matrices A_m, A_{jk} of A defined at the beginning of §1.2. The Routh-Hurwitz criterion says that A is stable, i.e., all of the roots of $P(\lambda)$ are in the left half complex plane, if and only if

$$p_1 > 0, \quad p_3 > 0, \quad p_1 p_2 - p_3 > 0. \tag{2.1}$$

Note that these conditions imply $p_2 > 0$.

We denote by $P(\lambda; \mu) = \lambda^3 + p_1(\mu)\lambda^2 + p_2(\mu)\lambda + p_3(\mu)$ the characteristic polynomial of $-\mu D + A$. The coefficients $p_j(\mu)$ $(j = 1, 2, 3)$ are given by

$$\begin{aligned} p_1(\mu) &= \mathrm{tr}(\mu D - A), \quad p_3(\mu) = \det(\mu D - A), \\ p_2(\mu) &= \det(A_{12} - \mu D_{12}) + \det(A_{23} - \mu D_{23}) + \det(A_{13} - \mu D_{13}), \end{aligned}$$

which lead us to:

$$\begin{aligned} p_1(\mu) &= p_1 + (d_1 + d_2 + d_3)\mu, \\ p_2(\mu) &= p_2 + [-(\mathrm{tr}\, A_{23})d_1 - (\mathrm{tr}\, A_{13})d_2 - (\mathrm{tr}\, A_{12})d_3]\mu \\ &\qquad + [d_1 d_2 + d_2 d_3 + d_3 d_1]\mu^2, \end{aligned} \tag{2.2}$$

$$p_3(\mu) = p_3 + [(\det A_{23})d_1 + (\det A_{13})d_2 + (\det A_{12})d_3]\mu + [-A_3 d_1 d_2 - A_2 d_1 d_3 - A_1 d_2 d_3]\mu^2 + d_1 d_2 d_3 \mu^3, \tag{2.3}$$

$$\begin{aligned} & p_1(\mu)p_2(\mu) - p_3(\mu) \\ &= p_1 p_2 - p_3 + [(\det A_{12} + \det A_{13} + (\operatorname{tr} A)(\operatorname{tr} A_{23}))d_1 \\ &\quad + (\det A_{12} + \det A_{23} + (\operatorname{tr} A)(\operatorname{tr} A_{13}))d_2 \\ &\quad + (\det A_{23} + \det A_{13} + (\operatorname{tr} A)(\operatorname{tr} A_{12}))d_3]\mu \\ &\quad + [-(\operatorname{tr} A_{23})d_1^2 - (\operatorname{tr} A_{13})d_2^2 - (\operatorname{tr} A_{12})d_3^2 \\ &\quad - 2(\operatorname{tr} A)(d_1 d_2 + d_1 d_3 + d_2 d_3)]\mu^2 \\ &\quad + [2d_1 d_2 d_3 + d_1^2(d_2 + d_3) + d_2^2(d_1 + d_3) + d_3^2(d_1 + d_2)]\mu^3. \end{aligned} \tag{2.4}$$

We apply the negation of Routh-Hurwitz criterion (2.1) to $p_j(\mu)$ $(j = 1, 2, 3)$ to show that $P(\lambda; \mu)$ has roots $\lambda(\mu)$ with non-negative real part for some $\mu > 0$. Since $p_1(\mu) > 0$ for all $\mu \geq 0$ in (2.2), the real part of $\lambda(\mu)$ possibly becomes positive only by violating one of the other two inequalities in (2.1), namely,

$$p_3(\mu) \leq 0 \quad \text{or} \quad p_1(\mu)p_2(\mu) - p_3(\mu) \leq 0 \quad \text{for some } \mu > 0.$$

It is elementary to prove:

(S) If $p_3(\mu)$ changes its sign from positive to negative as $\mu > 0$ varies with $p_1(\mu)p_2(\mu) - p_3(\mu)$ being positive, then one of $\lambda(\mu)$ changes its sign from negative to positive along the real axis.

(W) If $p_1(\mu)p_2(\mu) - p_3(\mu)$ changes its sign from positive to negative as $\mu > 0$ varies with $p_3(\mu)$ being positive, then a non-real root $\lambda(\mu)$ and its complex conjugate in pair cross the imaginary axis from left to right.

According to Definition 1.1, the statements (S) and (W) correspond, respectively, to *primary* S-instability and *primary* W-instability. In the proof of Theorem 1.1 below, we do not bother verifying additional conditions "*with* $p_1(\mu)p_2(\mu) - p_3(\mu)$ *being positive*" and "*with* $p_3(\mu)$ *being positive*", respectively, for (S) and (W). This is allowed, because we do not claim in Theorem 1.1 that S-instability and W-instability be primary.

By exchanging rows and columns appropriately, we may assume without loss of generality that $j = 1$, $k = 2$ and $m = 3$.

Proof of Theorem 1.1 (i): For fixed $d_1 > 0$, $d_2 > 0$ we set $d_3 = 0$, then $p_3(\mu)$ in (2.3) reduces to

$$p_3(\mu) = p_3 + [(\det A_{23})d_1 + (\det A_{13})d_2]\mu - A_3 d_1 d_2 \mu^2, \tag{2.5}$$

and A_3 being unstable and A being stable, we have $A_3 > 0$, $p_3 > 0$. Therefore, regardless of the sign of the coefficient of μ, there exists $\mu^* > 0$ so that $p_3(\mu) > 0$ for $0 \leq \mu < \mu^*$ and $p_3(\mu) < 0$ for $\mu > \mu^*$. We now perturb $d_3 > 0$ off from $d_3 = 0$. Then there exist $\underline{\mu} > 0$, $\bar{\mu} > 0$ with $\underline{\mu} < \bar{\mu}$ such that $p_3(\mu) > 0$ for $0 \leq$

$\mu < \underline{\mu}$ or $\mu > \bar{\mu}$, and $p_3(\mu) < 0$ for $\underline{\mu} < \mu < \bar{\mu}$. Therefore, when $d_3 \ll \min\{d_1, d_2\}$, S-instability occurs for $\mu \in (\underline{\mu}, \bar{\mu})$.

Proof of Theorem 1.1 (ii): For fixed $d_3 > 0$ we set $d_1 = d_2 = 0$, then $p_1(\mu)p_2(\mu) - p_3(\mu)$ in (2.4) reduces to

$$p_1(\mu)p_2(\mu) - p_3(\mu) = p_1p_2 - p_3 + [\det A_{23} + \det A_{13} + (\mathrm{tr}\, A)(\mathrm{tr}\, A_{12})]d_3\mu - (\mathrm{tr}\, A_{12})d_3^2\mu^2, \tag{2.6}$$

and A_{12} being type-1 unstable and A being stable, we have $\mathrm{tr}\, A_{12} > 0$, $p_1p_2 - p_3 > 0$. Therefore, regardless of the sign of the coefficient of μ, there exists $\mu^* > 0$ so that $p_1(\mu)p_2(\mu) - p_3(\mu) > 0$ for $0 \le \mu < \mu^*$ and $p_1(\mu)p_2(\mu) - p_3(\mu) < 0$ for $\mu > \mu^*$. We now perturb $d_1 > 0$, $d_2 > 0$ off from $d_1 = d_2 = 0$. Then there exist $\underline{\mu} > 0$, $\bar{\mu} > 0$ with $\underline{\mu} < \bar{\mu}$ such that $p_1(\mu)p_2(\mu) - p_3(\mu) > 0$ for $0 \le \mu < \underline{\mu}$ or $\mu > \bar{\mu}$, and $p_1(\mu)p_2(\mu) - p_3(\mu) < 0$ for $\underline{\mu} < \mu < \bar{\mu}$. This means that W-instability occurs for $\mu \in (\underline{\mu}, \bar{\mu})$ when $d_3 \gg \max\{d_1, d_2\}$.

Proof of Theorem 1.1 (iii): For fixed $d_3 > 0$ we set $d_1 = d_2 = 0$, then $p_3(\mu)$ in (2.3) reduces to

$$p_3(\mu) = p_3 + (\det A_{12})d_3\mu. \tag{2.7}$$

Now, A_{12} being type-2 unstable and A being stable, we have $\det A_{12} < 0$, $p_3 > 0$. Therefore, there exists $\mu^* > 0$ so that $p_3(\mu) > 0$ for $0 \le \mu < \mu^*$ and $p_3(\mu) < 0$ for $\mu > \mu^*$ in (2.7). We now perturb $d_1 > 0$, $d_2 > 0$ off from $d_1 = d_2 = 0$. Then there exist $\underline{\mu} > 0$, $\bar{\mu} > 0$ with $\underline{\mu} < \bar{\mu}$ such that $p_3(\mu) > 0$ for $0 \le \mu < \underline{\mu}$ or $\mu > \bar{\mu}$, and $p_3(\mu) < 0$ for $\underline{\mu} < \mu < \bar{\mu}$. This means that S-instability occurs for $\mu \in (\underline{\mu}, \bar{\mu})$ when $d_3 \gg \max\{d_1, d_2\}$.

Proof of Theorem 1.1 (iv): This is the combination of cases (ii) and (iii). For fixed $d_3 > 0$ we set $d_1 = d_2 = 0$, then $p_3(\mu)$ in (2.3) and $p_1(\mu)p_2(\mu) - p_3(\mu)$ in (2.4) reduce, respectively to (2.7) and (2.6). Since A_{12} is type-3 unstable and A is stable, we have $\mathrm{tr}\, A_{12} > 0$, $\det A_{12} < 0$, $p_3 > 0$ and $p_1p_2 - p_3 > 0$. Therefore, there exist $\mu_{\mathrm{s}} > 0$ and $\mu_{\mathrm{w}} > 0$ so that

$$p_3(\mu) > 0 \quad \text{for } 0 \le \mu < \mu_{\mathrm{s}} \qquad \text{and} \qquad p_3(\mu) < 0 \quad \text{for } \mu > \mu_{\mathrm{s}},$$
$$p_1(\mu)p_2(\mu) - p_3(\mu) > 0 \quad \text{for } 0 \le \mu < \mu_{\mathrm{w}} \qquad \text{and}$$
$$p_1(\mu)p_2(\mu) - p_3(\mu) < 0 \quad \text{for } \mu > \mu_{\mathrm{w}}.$$

By perturbing $d_1 > 0$, $d_2 > 0$ off from $d_1 = d_2 = 0$, S- and W-instability occur for suitable $\mu > 0$ when $\max\{d_1, d_2\} \ll d_3$.

Proof of Theorem 1.1 (v): Because A_3 (> 0) and A_{12} are unstable and A is stable, we must have $\mathrm{tr}\, A_{12} < 0$, implying that A_{12} is type-2 unstable and $p_3 > 0$. For fixed $d_3 > 0$ we set $d_1 = d_2 = 0$, then $p_3(\mu)$ in (2.3) reduces to (2.7). For fixed $d_1 > 0$, $d_2 > 0$ we set $d_3 = 0$, then $p_3(\mu)$ in (2.3) reduces to (2.5). The remaining reasoning is the same as that for the proof of Theorem 1.1 (iii) for (a), or of Theorem 1.1 (i) for (b).

Proof of Theorem 1.2 (i): The conditions imposed on the sub-matrices imply that $A_m < 0$ $(m = 1, 2, 3)$, $\operatorname{tr} A_{jk} < 0$, $\det A_{jk} > 0$ $(0 \le j < k \le 3)$ and $\operatorname{tr} A < 0$. From these inequality, we easily find that $p_3(\mu) > 0$ in (2.3) and $p_1(\mu)p_2(\mu) - p_3(\mu) > 0$ in (2.4) for all possible $\mu > 0$ and $d_j > 0$ $(j = 1, 2, 3)$, because the coefficients of μ^0, μ, μ^2 and μ^3 are positive. Therefore, Turing instability does not occur.

Proof of Theorem 1.2 (ii): The conditions imposed on the 2-component sub-matrices imply that $\operatorname{tr} A_{jk} < 0$, $\det A_{jk} > 0$ $(0 \le j < k \le 3)$ and $\operatorname{tr} A < 0$. From these inequality, we easily find that $p_1(\mu)p_2(\mu) - p_3(\mu) > 0$ in (2.4) for all possible $\mu \ge 0$ and $d_j \ge 0$ $(j = 1, 2, 3)$, because $p_1p_2 - p_3 > 0$ and the coefficients of μ, μ^2 and μ^3 are non-negative. Therefore, W-instability does not occur.

Proof of Theorem 1.2 (iii): Since A is stable and A_{12} is type-2 unstable, we have that $\det A_{23} + \det A_{13} > 0$ and $\operatorname{tr} A_{12} < 0$. For fixed $d_3 > 0$ and $d_1 = d_2 = 0$, we have $p_1(\mu)p_2(\mu) - p_3(\mu) > 0$ in (2.6) for all $\mu \ge 0$, which remains the same even after we perturb $d_1 > 0$, $d_2 > 0$ off from $d_1 = d_2 = 0$. Therefore, W-instability does not occur for $\max\{d_1, d_2\} \ll d_3$.

If, moreover, A_{13} and A_{23} are stable, in (2.4) the coefficients of μ^0, μ^2 and μ^3 are positive for all $d_j > 0$ $(j = 1, 2, 3)$. On the other hand, within the coefficient of μ in (2.4), the coefficient of d_3 is positive. If the coefficients of d_1, d_2 are positive, then the coefficient of μ in (2.4) is also positive and we have $p_1(\mu)p_2(\mu) - p_3(\mu) > 0$ for all $\mu \ge 0$ and $d_j \ge 0$ $(j = 1, 2, 3)$. If the coefficients of d_1 and d_2 are negative, then for $\max\{d_1, d_2\} \le d_3$ we have [coefficient of μ in (2.4)] $\ge 2(p_2 + p_1^2)d_3 > 0$. If the coefficient of d_1 is negative and that of d_2 is non-negative, then for $\max\{d_1, d_2\} \le d_3$ we have that the coefficient of μ in (2.4) is estimated from below as follows

$$\begin{aligned}[\text{coefficient of } \mu \text{ in (2.4)}] \ge{}& \{p_2 + \det A_{13} + (\operatorname{tr} A)(\operatorname{tr} A_{23} + \operatorname{tr} A_{13})\}d_3 \\ &+ \{\det A_{12} + \det A_{23} + (\operatorname{tr} A)(\operatorname{tr} A_{13})\}d_2 > 0,\end{aligned}$$

which implies that W-instability does not occur. The arguments are similar if the coefficient of d_1 is non-negative and that of d_2 is negative. Therefore, we conclude that W-instability is impossible for $\max\{d_1, d_2\} \le d_3$.

Proof of Theorem 1.2 (iv): We first show that the coefficient of μ in (2.3) is positive under the conditions $\max\{d_1, d_2\} \le d_3$ and $d_2 \le (-A_2/A_1)d_1$. If (1) is the case, the coefficient of μ is estimated from below by $p_2d_3 > 0$. Since $\operatorname{tr} A_{12} > 0$, we have $A_1 > |A_2|$ and hence $d_2 \le (-A_2/A_1)d_1 < d_1$. Therefore, if (2) is the case, then the coefficient is estimated by $p_2d_2 > 0$. Since $A_3 < 0$, the coefficient of μ^2 is estimated from below by $-A_2d_1d_3 - A_1d_2d_3$ which is positive if $d_2 < (-A_2/A_1)d_1$. All coefficients of $p_3(\mu)$ in (2.3) are positive, and therefore, S-instability does not occur for $\max\{d_1, d_2\} \le d_3$, $d_2 \le (-A_2/A_1)d_1$.

Proof of Theorem 1.2 (v): We have $A_3 < 0$, $A_1 > 0$ and $A_2 > 0$.

If (1) is the case, for $\max\{d_1, d_2\} \le d_3$, $p_3(\mu)$ in (2.3) is estimated from below:

$$p_3(\mu) \ge p_3 + d_3[\det A_{12} - (A_2 d_1 + A_1 d_2)\mu + d_1 d_2 \mu^2]\mu.$$

The minimum value of the quadratic function of $\mu \ge 0$ inside the bracket $[\cdots]$ is given by

$$\det A_{12} - \frac{(A_2 d_1 + A_1 d_2)^2}{4 d_1 d_2}.$$

We will now show that the minimum value is nonnegative along half lines $d_2 = \ell d_1$ $(d_1 > 0)$ for suitable $\ell > 0$. Namely, we will find $\ell > 0$ so that

$$\det A_{12} - \frac{(A_2 + A_1 \ell)^2}{4\ell} \ge 0.$$

Thanks to the condition $\det A_{12} > A_1 A_2$, this is certainly true for $\ell = A_2/A_1$. We easily find that this inequality is satisfied for $\ell \in [\ell_1, \ell_2]$, where ℓ_1 and ℓ_2 are roots of the quadratic equation $(A_1 \ell + A_2)^2 = 4\ell \det A_{12}$ with $0 < \ell_1 < A_2/A_1 < \ell_2$.

If (2) is the case, for $\max\{d_1, d_2\} \le d_3$, $p_3(\mu)$ in (2.3) is estimated from below:

$$p_3(\mu) \ge p_3 + d_3[p_2 - (A_2 d_1 + A_1 d_2)\mu + d_1 d_2 \mu^2]\mu.$$

The minimum value of the quadratic function of $\mu \ge 0$ inside the bracket $[\cdots]$ is given by

$$p_2 - \frac{(A_2 d_1 + A_1 d_2)^2}{4 d_1 d_2}.$$

The remaining arguments are similar to those for (1). This completes the proof.

3. Examples

In this section, we display explicit examples of A to which Theorems 1.1, 1.2 and Corollary 1.1 apply. We then take up a model called the extended Brusselator ([19]) and numerically study this model from the viewpoint of Turing bifurcations.

3.1. Illustrative examples. We exhibit examples of A to which Theorem 1.1 applies. The examples below are chosen so that the number of unstable subsystems is minimum, and hence the instability in each statement of Theorem 1.1 is mostly primary. In the subsequent figures, the white (resp. gray) area in d_j-d_k planes indicates the area where $p_3(\mu)$ or $p_1(\mu)p_2(\mu) - p_3(\mu)$ is positive (resp. negative). Therefore, the boundary between the white and gray areas is the location where S- or W-instability actually sets in for suitable eigenvalues $\mu > 0$ of the Laplace operator.

(i) This is an example for Theorem 1.1 (i):

$$A = \begin{pmatrix} -2 & 0 & 1 \\ 1 & -1 & -1 \\ -3 & 2 & 0.5 \end{pmatrix}$$

which is a stable matrix, because the stability conditions

$$p_1 = 2.5 > 0, \quad p_2 = 5.5, \quad p_3 = 4 > 0, \quad p_1p_2 - p_3 = 9.75 > 0$$

are satisfied. Complementary pairs are:

- $A_{12} = \begin{pmatrix} -2 & 0 \\ 1 & -1 \end{pmatrix}$: Stable, $A_3 = 0.5$: Unstable,
- $A_{13} = \begin{pmatrix} -2 & 1 \\ -3 & 0.5 \end{pmatrix}$: Stable, $A_2 = -1$: Stable,
- $A_{23} = \begin{pmatrix} -1 & -1 \\ 2 & 0.5 \end{pmatrix}$: Stable, $A_1 = -2$: Stable,

and Theorem 1.1 (i) applies with $j = 1$, $k = 2$, $m = 3$. Figure 1 below shows that S-instability occurs for small $d_3 > 0$.

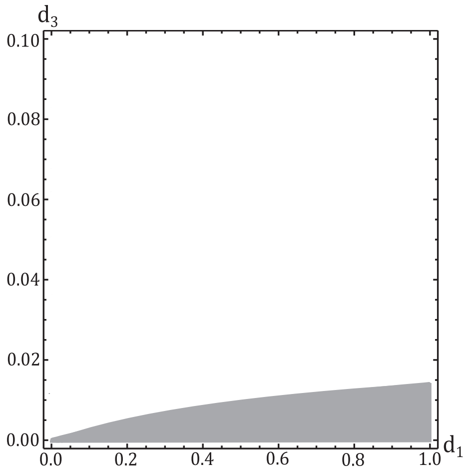

Figure 1. We set the parameter $d_2 = 1$ in Figure 1. The pair (d_1, d_3) in the white area means that $p_3(\mu) = d_1d_3\mu^3 + (-0.5d_1 + 2d_3 + d_1d_3)\mu^2 + (2 + 1.5d_1 + 2d_3)\mu + 4 > 0$ for all $\mu > 0$, while the pair (d_1, d_3) in the gray area indicates that $p_3(\mu) < 0$ for some $\mu > 0$. The S-instability occurs on the boundary between these two areas.

We may consider this case as a direct generalization of 2-component Turing instability to a 3-component version.

(ii) An example for Theorem 1.1 (ii) is given by

$$A = \begin{pmatrix} 2 & -3 & -4 \\ 1 & -1 & 1 \\ 2 & -1 & -3 \end{pmatrix}$$

whose stability conditions

$$p_1 = 2 > 0, \quad p_2 = 7, \quad p_3 = 11 > 0, \quad p_1 p_2 - p_3 = 3 > 0$$

are satisfied. Complementary pairs are

- $A_{12} = \begin{pmatrix} 2 & -3 \\ 1 & -1 \end{pmatrix}$: type-1 unstable, $A_3 = -3$: Stable,
- $A_{13} = \begin{pmatrix} 2 & -4 \\ 2 & -3 \end{pmatrix}$: Stable, $A_2 = -1$: Stable,
- $A_{23} = \begin{pmatrix} -1 & 1 \\ -1 & -3 \end{pmatrix}$: Stable, $A_1 = 2$: Unstable,

and Theorem 1.1 (ii) applies with $j = 1$, $k = 2$, $m = 3$. In this case, a 1-component unstable subsystem $(A_1 = 2)$ must appear, in addition to the type-1 unstable subsystem A_{12}. We cannot completely separate the interaction between the complementary pairs (A_{12}, A_3) and (A_1, A_{23}). In FIGURES 2 and 3 below, S-instability (on the left) is caused by the pair (A_1, A_{23}) as in (i), while W-instability (on the right) is due to the pair (A_{12}, A_3).

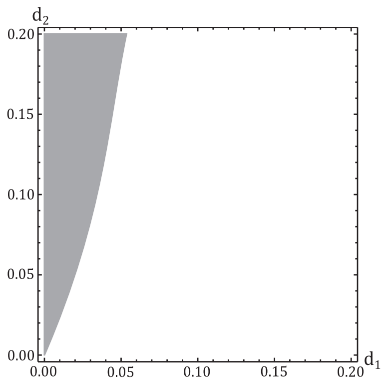

FIGURE 2

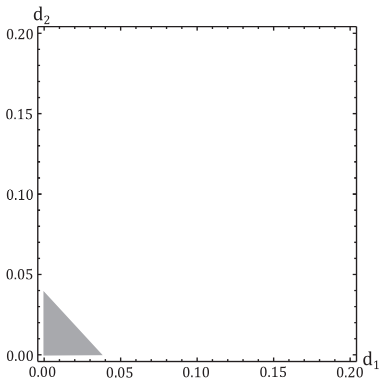

FIGURE 3

We set the parameter $d_3 = 1$ in FIGURES 2 and 3. In FIGURE 2, the pair (d_1, d_2) is in the white area if $p_3(\mu) = d_1 d_2 \mu^3 + (d_1 - 2d_2 + 3d_1 d_2)\mu^2 + (1 + 4d_1 + 2d_2)\mu + 11 > 0$ for all $\mu > 0$, and the pair is in the gray area if $p_3(\mu) < 0$ for some $\mu > 0$. S-instability occurs on the boundary between these areas. On the other hand, in FIGURE 3, (d_1, d_2) in the white area indicates that $p_1(\mu)p_2(\mu) - p_3(\mu) = \{d_1 + d_2 + 2d_1 d_2 + (1 + d_1)d_2^2 + d_1^2(1 + d_2)\}\mu^3 + \{-1 + 4d_1^2 + d_2^2 + 4(d_1 + d_2 + d_1 d_2)\}\mu^2 + (4 + 11d_1 + 7d_2)\mu + 3 > 0$ for all $\mu > 0$, while the pair in the gray area means that $p_1(\mu)p_2(\mu) - p_3(\mu) < 0$ for some $\mu > 0$. W-instability occurs on the boundary between these areas.

We may read off from the figures above that W-instability is primary for $d_2 < 2d_1$, while Corollary 1.1 (iii) guarantees that the primary W-instability occurs for $d_2 \le d_1/2$ with $\max\{d_1, d_2\} \ll d_3$.

(iii) Our example for Theorem 1.1 (iii) is given by

$$A = \begin{pmatrix} -1 & 1 & -3 \\ 2 & -1 & -5 \\ 2 & 1 & -1.5 \end{pmatrix}$$

which satisfies the stability conditions

$$p_1 = 3.5 > 0, \quad p_2 = 13, \quad p_3 = 25.5 > 0, \quad p_1 p_2 - p_3 = 20 > 0.$$

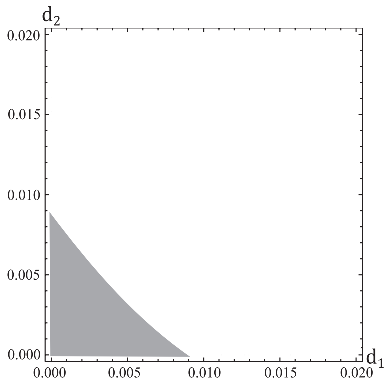

FIGURE 4. We set the parameter $d_3 = 1$ in FIGURE 4. The pair (d_1, d_2) in the white area means that $p_3(\mu) = d_1 d_2 \mu^3 + (d_1 + d_2 + 1.5 d_1 d_2)\mu^2 + (-1 + 6.5 d_1 + 7.5 d_2)\mu + 25.5 > 0$ for all $\mu > 0$, while the pair is in the gray area if $p_3(\mu) < 0$ for some $\mu > 0$. S-instability occurs on the boundary between these areas.

The complementary pairs are:

- (A_{12}: type-2 unstable, A_3: Stable),
- (A_{13}: Stable, A_2: Stable),
- (A_{23}: Stable, A_1: Stable),

and there is only one unstable subsystem A_{12} which is of type-2. In this example, S-instability appears primarily. We may also consider this situation as a direct generalization of 2-component Turing instability to a 3-component version.

(iv) As an example to illustrate the application of Theorem 1.1 (iv), we take the matrix

$$A = \begin{pmatrix} 2 & -a & -4 \\ 1 & -1 & 1 \\ 2 & -1 & -3 \end{pmatrix}$$

containing a parameter a. As in the case (ii), we necessarily have one unstable 1-component subsystem ($A_1 = 2$), in addition to a type-3 unstable subsystem.

The stability conditions for this matrix are

$$p_1 = 2 > 0, \quad p_2 = a + 4, \quad p_3 = 5a - 4 > 0, \quad p_1 p_2 - p_3 = 12 - 3a > 0,$$

which are fulfilled for $4/5 < a < 4$. For $4/5 < a < 2$, A_{12} is type-3 unstable and complementary pairs in A for this range of a are

- (A_{12}: type-3 unstable, A_3: Stable),
- (A_{13}: Stable, A_2: Stable),
- (A_{23}: Stable, A_1: Unstable).

There are three sources of instability in this system: One source is the 1-component subsystem $A_1 = 2$. The other two come from the type-3 unstable A_{12}. They are $\operatorname{tr} A_{12} > 0$ which tends to cause W-instability, and $\det A_{12} < 0$ which tends to cause S-instability. These three sources interact within the stable full system and exhibits varied manifestation of Turing instabilities. The decisive factor is the relative magnitude between $\operatorname{tr} A_{12}$ and $|\det A_{12}|$. In FIGURES 5 through 12 below, we show how the areas of S-instability and W-instability vary according to the values of a for (1) $a = 0.85$, (2) $a = 1$, (3) $a = 1.4$, (4) $a = 1.9$, which in turn adjust the relative magnitude between $\operatorname{tr} A_{12}$ and $|\det A_{12}|$.

(1) In this case, the S-instability originating from $\det A_{12} < 0$ is dominant, and W-instability does not manifest primarily. The potential W-instability area (the gray in FIGURE 6, below) is completely contained in the gray area in the left figure, below.

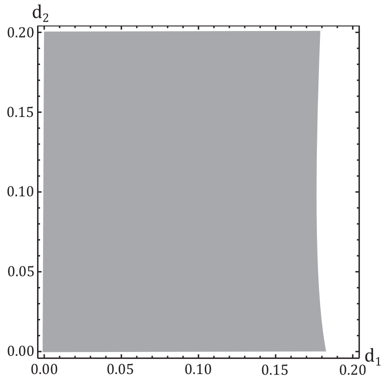

FIGURE 5

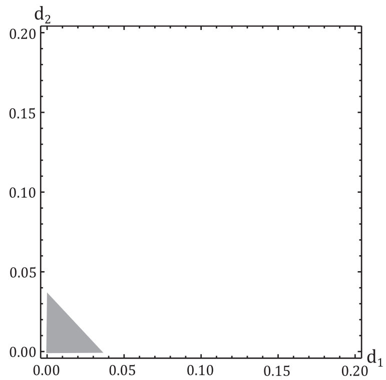

FIGURE 6

In FIGURES 5 and 6, we set the parameters $d_3 = 1$, $a = 0.85$ which imply $|\operatorname{tr} A_{12}|(= 1) < |\det A_{12}|(= 1.15)$. In FIGURE 5, the pair (d_1, d_2) in the white area means that $p_3(\mu) = d_1 d_2 \mu^3 + (d_1 + 2d_2 + 3d_1 d_2)\mu^2 + (-1.15 + 4d_1 + 2d_2)\mu + 0.25 > 0$ for all $\mu > 0$, while the pair in the gray area means that $p_3(\mu) < 0$ for some $\mu > 0$. S-instability occurs on the boundary between these areas. On the other hand, in FIGURE 6, the pair is in the white area if $p_1(\mu)p_2(\mu) - p_3(\mu) = \{d_1 + d_2 + 2d_1 d_2 + (1 + d_1)d_2^2 + d_1^2(1 + d_2)\}\mu^3 + \{-1 + 4d_1^2 + d_2^2 + 4(d_1 + d_2 + d_1 d_2)\}\mu^2 + (4 + 8.85d_1 + 4.85d_2)\mu + 9.45 > 0$ for all $\mu > 0$, and the pair is in the gray area if $p_1(\mu)p_2(\mu) - p_3(\mu) < 0$ for some $\mu > 0$. W-instability occurs on the boundary between these areas.

(2) In this case, the instability effect due to the unstable-stable pair (A_1, A_{23}) gained more influence than the instability $\det A_{12} < 0$ and S-instability is primary, while W-instability is not yet observable.

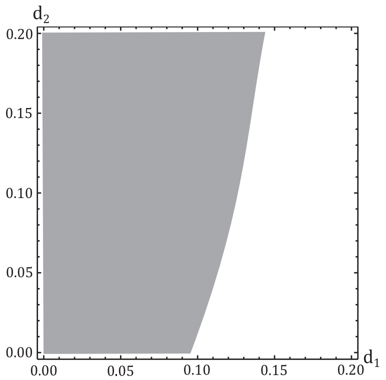

FIGURE 7

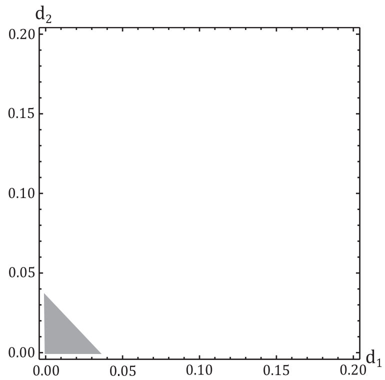

FIGURE 8

We set parameters $d_3 = 1$, $a = 1.0$ for which we have $|\mathrm{tr}\, A_{12}| = |\det A_{12}|$. In FIGURE 7, (d_1, d_2) in the white area represents that $p_3(\mu) = d_1 d_2 \mu^3 + (d_1 - 2d_2 + 3d_1 d_2)\mu^2 + (-1 + 4d_1 + 2d_2)\mu + 1 > 0$ for all $\mu > 0$, and the pair is in the gray area if $p_3(\mu) < 0$ for some $\mu > 0$. On the other hand, in FIGURE 8, the pair (d_1, d_2) in the white area means that $p_1(\mu)p_2(\mu) - p_3(\mu) = \{d_1 + d_2 + 2d_1 d_2 + (1 + d_1)d_2^2 + d_1^2(1 + d_2)\}\mu^3 + \{-1 + 4d_1^2 + d_2^2 + 4(d_1 + d_2 + d_1 d_2)\}\mu^2 + (4 + 9d_1 + 5d_2)\mu + 9 > 0$ for all $\mu > 0$, while the pair is in the gray area if $p_1(\mu)p_2(\mu) - p_3(\mu) < 0$ for some $\mu > 0$.

(3) In this case, S-instability effect due to $\det A_{12} < 0$ further decreases and W-instability occurs primarily in some area.

(4) In this case, the area of primary W-instability increases, and S-instability is mainly caused by the pair (A_1, A_{23}), while the effects due to $\det A_{12} < 0$ seems to be negligible.

More detailed computations reveal that W-instability starts to occur for $a \approx 1.3$ and larger. We computed values (d_1, d_2) for which both S-instability and W-instability simultaneously occur for $a = 1.3, 1.4, 1.408, 1.41, 1.9$. We also computed the corresponding critical wave numbers κ_S, κ_W. The result is summarized in TABLE 1.

When $\mathrm{tr}\, A_{12} < |\det A_{12}|$, we have $\kappa_S < \kappa_W$ for which, however, S-instability tends to be primary and W-instability is hidden. On the other hand, when $\mathrm{tr}\, A_{12} > |\det A_{12}|$, we have $\kappa_S > \kappa_W$ for which both S-instability and W-instability occur. This is why it is reckoned that $\kappa_S > \kappa_W$ is a rule. Notice, however, for $a = 1.3$ we have $\kappa_W > \kappa_S$.

(v) We apply Theorem 1.1 (v) to the matrix

$$A = \begin{pmatrix} -1 & -2 & -1 \\ -1 & -1 & -2 \\ 1 & 3 & 0.5 \end{pmatrix}$$

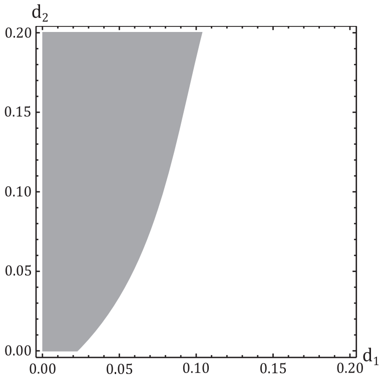

FIGURE 9

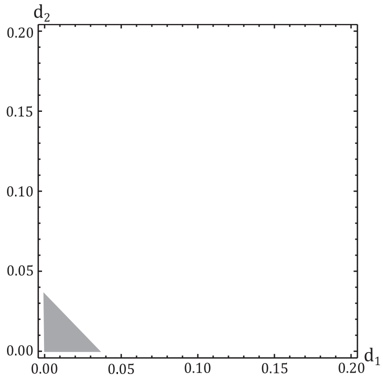

FIGURE 10

We set the parameters $d_3 = 1$, $a = 1.4$ which implies that $|\mathrm{tr}\, A_{12}| > |\det A_{12}|(= 0.6)$. In FIGURE 9, the pair (d_1, d_2) in the white area means that $p_3(\mu) = d_1 d_2 \mu^3 + (d_1 - 2d_2 + 3d_1 d_2)\mu^2 + (-0.6 + 4d_1 + 2d_2)\mu + 3 > 0$ for all $\mu > 0$, while the pair in the gray area means that $p_3(\mu) < 0$ for some $\mu > 0$. In FIGURE 10, the pair is in the white area if $p_1(\mu)p_2(\mu) - p_3(\mu) = \{d_1 + d_2 + 2d_1 d_2 + (1 + d_1)d_2^2 + d_1^2(1 + d_2)\}\mu^3 + \{-1 + 4d_1^2 + d_2^2 + 4(d_1 + d_2 + d_1 d_2)\}\mu^2 + (4 + 9.4d_1 + 5.4d_2)\mu + 7.8 > 0$ for all $\mu > 0$, and it is in the gray area if $p_1(\mu)p_2(\mu) - p_3(\mu) < 0$ for some $\mu > 0$.

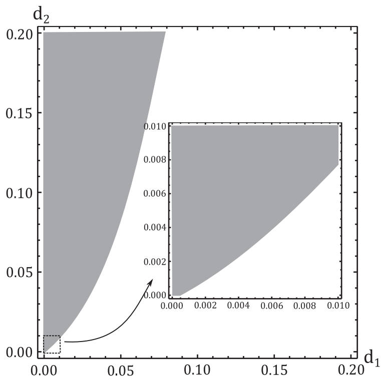

FIGURE 11

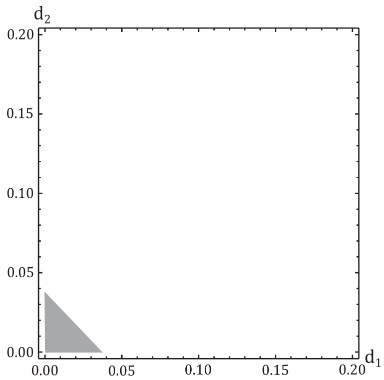

FIGURE 12

The parameters are set as $d_3 = 1$, $a = 1.9$ for which we have $|\mathrm{tr}\, A_{12}|(= 1) \gg |\det A_{12}|(= 0.1)$. In FIGURE 11, the pair is in the white area if $p_3(\mu) = d_1 d_2 \mu^3 + (d_1 - 2d_2 + 3d_1 d_2)\mu^2 + (-0.1 + 4d_1 + 2d_2)\mu + 5.5 > 0$ for all $\mu > 0$, and it is in the gray area if $p_3(\mu) < 0$ for some $\mu > 0$. In FIGURE 12, (d_1, d_2) in the white area represents that $p_1(\mu)p_2(\mu) - p_3(\mu) = \{d_1 + d_2 + 2d_1 d_2 + (1 + d_1)d_2^2 + d_1^2(1 + d_2)\}\mu^3 + \{-1 + 4d_1^2 + d_2^2 + 4(d_1 + d_2 + d_1 d_2)\}\mu^2 + (4 + 9.9d_1 + 5.9d_2)\mu + 6.3 > 0$ for all $\mu > 0$, and the pair in the gray area means that $p_1(\mu)p_2(\mu) - p_3(\mu) < 0$ for some $\mu > 0$. From these figures we can clearly identify the existence of a point (d_1, d_2) where both S-instability and W-instability simultaneously occur.

TABLE 1

a	1.3	1.4	1.408	1.41	1.9
d_1	0.0338445	0.0288521	0.0285321	0.0284537	0.0184498
d_2	0.00143095	0.00664213	0.00697764	0.00705998	0.0178036
κ_S	2.973	3.404	3.507	3.517	5.7
κ_W	3.521	3.507	3.508	3.507	3.404
relation	$\kappa_S < \kappa_W$	$\kappa_S < \kappa_W$	$\kappa_S \fallingdotseq \kappa_W$	$\kappa_S > \kappa_W$	$\kappa_S > \kappa_W$

whose stability conditions

$$p_1 = 1.5 > 0, \quad p_2 = 5, \quad p_3 = 0.5 > 0, \quad p_1 p_2 - p_3 = 7 > 0$$

are satisfied. Complementary pairs in this matrix are
- (A_{12}: type-2 unstable, $A_3 = 0.5$: Unstable),
- (A_{13}: Stable, $A_2 = -1$: Stable),
- (A_{23}: Stable, $A_1 = -1$: Stable).

FIGURE 13 shows S-instability associated with type-2 unstable A_{12}, while FIGURE 14 below shows the instability associated with the 1-component unstable subsystem A_3.

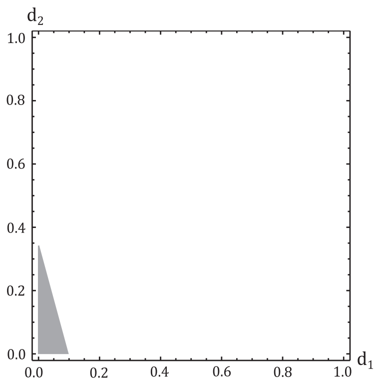

FIGURE 13

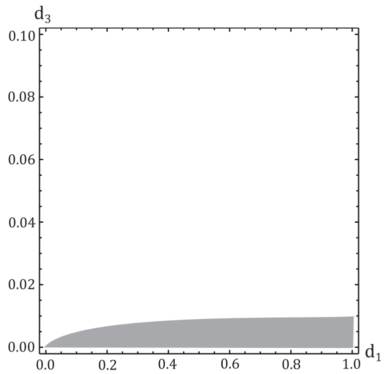

FIGURE 14

We set $d_3 = 1$ in FIGURE 13 and $d_2 = 1$ in FIGURE 14. FIGURE 13 represents that (d_1, d_2) is in the white area if $p_3(\mu) = d_1 d_2 \mu^3 + (d_1 + d_2 + 0.5 d_1 d_2)\mu^2 + (-1 + 5.5 d_1 + 0.5 d_2)\mu + 0.5 > 0$ for all $\mu > 0$, and it is in the gray area otherwise. In FIGURE 14, the pair (d_1, d_3) is in the white area if $p_3(\mu) = d_1 d_3 \mu^3 + (-0.5 d_1 + d_3 + d_1 d_3)\mu^2 + (0.5 + 5.5 d_1 - d_3)\mu + 0.5 > 0$ for all $\mu > 0$, and it is in the gray area otherwise. S-instability occurs on the boundary between these areas.

We have shown the simplest example for each statement of Theorem 1.1. Many examples in application may contain more unstable subsystems than the examples above, and the Turing instabilities caused by these unstable subsystems interact to produce complicated bifurcation phenomena. We will present some of such examples in the next subsection and in §4.

3.2. Extended Brusselator Model. The Extended Brusselator Model is the following system of reaction-diffusion equations ([19]).

$$\begin{cases} \dfrac{\partial u}{\partial t} = d_1 \triangle u + p - (2+q)u + u^2 v + w, \\ \dfrac{\partial v}{\partial t} = d_2 \triangle v + qu - u^2 v, \\ \dfrac{\partial w}{\partial t} = d_3 \triangle w + u - w, \end{cases} \tag{3.1}$$

where $p > 0$ and $q > 0$ are real parameters. We easily find the unique homogeneous steady state $(u_0, v_0, w_0) = (p, q/p, p)$ of (3.1). The linearized reaction matrix A is given by

$$A = \begin{pmatrix} q-2 & p^2 & 1 \\ -q & -p^2 & 0 \\ 1 & 0 & -1 \end{pmatrix}. \tag{3.2}$$

In the first quadrant of the p-q parameter plane, we identify the region where A is stable, and subdivide the region into subregions according to the number and type of subsystems in A. Let $\lambda^3 + p_1\lambda^2 + p_2\lambda + p_3$ be the characteristic polynomial of A. The stability conditions are given by

$$\begin{aligned} &p_1 = p^2 - q + 3 > 0, \quad p_3 = p^2 > 0, \\ &p_1 p_2 - p_3 = q^2 - 4(p^2+2)q + 3(p^4 + 3p^2 + 1) > 0. \end{aligned}$$

The third condition is equivalent to $(q > q_+(p), p > 0)$ or $(0 < q < q_-(p), p > 0)$, where $q_\pm(p)$ are two roots of $p_1 p_2 - p_3 = 0$ as a quadratic equation in q. However, the region $q > q_+(p)$ is eliminated from the stability region of A by the requirement $p_1 > 0$ ($\Leftrightarrow q < p^2 + 3$), as we verify $q_+(p) \geq p^2 + 3$ for $p > 0$. Therefore the stability region of A is $\{(p,q) \mid p > 0, 0 < q < q_-(p)\}$.

We notice that subsystems A_2, A_3 and A_{23} are stable for all parameter values $p > 0$, $q > 0$. Stability or instability of other subsystems is determined as follows.

- A_1 is stable if $q < 2$, and unstable if $q > 2$.
- A_{12} is stable if $q < p^2 + 2$, and is type-1 unstalbe if $q > p^2 + 2$.
- A_{13} is stable if $0 < q < 1$, is type-2 unstable if $1 < q < 3$, and is type-3 unstable if $q > 3$.

Figure 15 below shows the stability region of A and its subregions. The subregions are defined by

(I) $\{(p,q)\,|\,0 < p, 0 < q < 1\}$, (II) $\{(p,q)\,|\,0 < p, 1 < q < \min[2, q_-(p)]\}$,
(III) $\{(p,q)\,|\,0 < p, 2 < q < \min[3, q_-(p)]\}$, (IV) $\{(p,q)\,|\,1 < p, 3 < q < p^2 + 2\}$,
(V) $\{(p,q)\,|\,1 < p, p^2 + 2 < q < q_-(p)\}$.

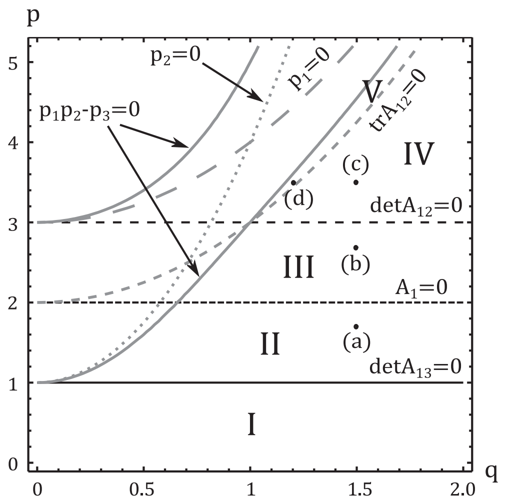

FIGURE 15

The number of unstable subsystems in A varies from regions (I) to (V), as follows.

- Region I $\cdots$ All subsystems of A are stable (no unstable subsystem).
- Region II $\cdots$ A_{13} is type-2 unstable.
- Region III $\cdots$ A_1 is unstable and A_{13} is type-2 unstable.
- Region IV $\cdots$ A_1 is unstable and A_{13} is type-3 unstable.
- Region V $\cdots$ A_1 is unstable, A_{12} is type-1 unstable and A_{13} is type-3 unstable.

In Region I, Theorem 1.2 (i) applies, where Turing instability never occurs for any choice of the diffusion matrix D. In Regions II and III, Theorem 1.1 (iii) applies to the complementary unstable-stable pair A_{13}-A_2. If d_1 and d_3 are sufficiently small compared with d_2, then S-instability occurs. In Region IV, Theorem 1.1 (iv) applies to the pair A_{13}-A_2. If d_2 is sufficiently large compared with d_1 and d_3, then either S- or W-instability occurs, or both S- and W-instabilities occur. In Region V, Theorem 1.1 (ii) and (iv) apply to the complementary unstable-stable pairs A_{12}-A_3 and A_{13}-A_2, respectively. If d_1 and d_2 are sufficiently small compared with d_3, then W-instability occurs. If d_1 and d_3 are sufficiently small compared with d_2, then either S-instability or W-instability occurs, or both S- and W-instabilities occur.

In order to improve the qualitative descriptions of Turing instabilities in Regions II, III, IV and V, we pick one point from each region as indicated by (a), (b), (c) and (d) in FIGURE 15. We now numerically detect the diffusion matrix D for which Turing instabilities occur, with the restriction $d_1 + d_2 + d_3 = 1$. The corresponding results are shown in FIGURES 16 through 20, where we project the diffusion coefficients (d_1, d_2, d_3) onto the d_1-d_3 plane. In FIGURES 16 through 20, meaningful points (d_1, d_3) are those satisfying $0 \le d_1, d_3, d_1 + d_3 \le 1$, hence the upper-right triangular gray regions should be neglected. The homogeneous steady state is stable for (d_1, d_3) in white area and unstable for (d_1, d_3) in black area, with respect to S-mode and W-mode, respectively.

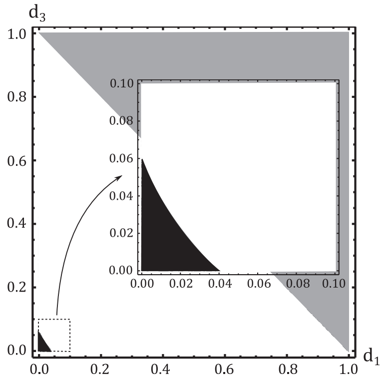

FIGURE 16

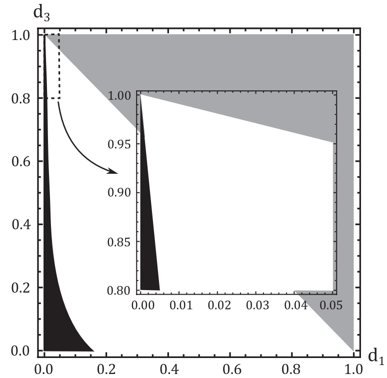

FIGURE 17

FIGURE 16 is for the parameter values $(p, q) = (1.5, 1.7)$. The pair (d_1, d_3) is in the white area if $p_3(\mu) = d_1 d_3(1 - d_1 - d_3)\mu^3 + \{d_1(1 - d_1) + 0.95 d_1 d_3 + d_3(1 - d_3)\}\mu^2 + (-0.7 + 2.95 d_1 + 5.2 d_3)\mu + 2.25 > 0$ for all $\mu > 0$, and it is in the black area if $p_3(\mu) < 0$ for some $\mu > 0$. FIGURE 17 is for the parameter values $(p, q) = (1.5, 2.7)$. The pair (d_1, d_3) is in the white area if $p_3(\mu) = d_1 d_3(1 - d_1 - d_3)\mu^3 + \{d_1(1 - d_1) + 1.95 d_1 d_3 - 0.7 d_3(1 - d_3)\}\mu^2 + (-1.7 + 3.95 d_1 + 6.2 d_3)\mu + 2.25 > 0$ for all $\mu > 0$, and it is in the black area otherwise.

FIGURE 16 indicates S-instability associated with type-2 unstable A_{13}, while FIGURE 17 shows S-instability region caused both by type-2 unstable A_{13} and unstable subsystem A_1.

Both of FIGURES 18 and 19 show the S-instability caused by the combined effects of type-3 unstable A_{13} and unstable subsystem A_1.

In FIGURE 20, the instability indicated in the upper-left corner is W-instability caused by the type-1 unstable A_{12}, while the instability indicated in the lower-left is the potential W-instability caused by the type-3 unstable A_{13}. However, the latter W-instability is not observed, because it is completely consumed inside the S-instability region in FIGURE 19.

3.3. Simulations for nonlinear equation. We solve the nonlinear equations (3.1) numerically with the initial conditions near the equilibrium state $(p, q/p, p)$ for the parameter values used in (a), (b), (c) and (d) above. These simulations reveal that Turing bifurcations actually take place near the instability

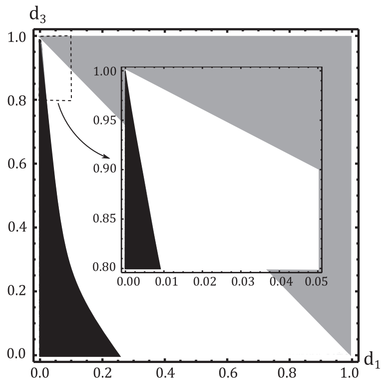

FIGURE 18

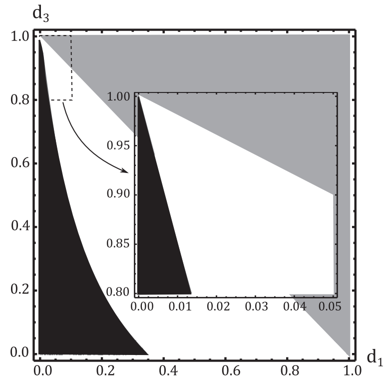

FIGURE 19

FIGURE 18 is for the parameter values $(p,q) = (1.5, 3.5)$. The pair (d_1, d_3) in the white area indicates that $p_3(\mu) = d_1 d_3(1 - d_1 - d_3)\mu^3 + \{d_1(1 - d_1) + 2.75 d_1 d_3 - 1.5 d_3(1 - d_3)\}\mu^2 + (-2.5 + 4.75 d_1 + 7d_3)\mu + 2.25 > 0$ for all $\mu > 0$. The pair is in the black area if $p_3(\mu) < 0$ for some $\mu > 0$. In FIGURE 19, the parameters are set as $(p,q) = (1.2, 3.5)$. If $p_3(\mu) = d_1 d_3(1 - d_1 - d_3)\mu^3 + \{d_1(1 - d_1) + 1.94 d_1 d_3 - 1.5 d_3(1 - d_3)\}\mu^2 + (-2.5 + 3.94 d_1 + 5.38 d_3)\mu + 1.44 > 0$ for all $\mu > 0$, then (d_1, d_3) is in the white area, and it is in the black area if $p_3(\mu) < 0$ for some $\mu > 0$.

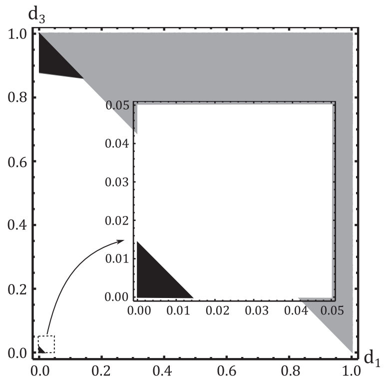

FIGURE 20. We set $(p,q) = (1.2, 3.5)$ in FIGURE 20. The pair (d_1, d_3) is in the white area if $p_1(\mu)p_2(\mu) - p_3(\mu) = (d_1 - d_1^2 + d_3 - 2d_1 d_3 + d_1^2 d_3 - d_3^2 + d_1 d_3^2)\mu^3 + (-0.5 + 2.88 d_1 + 0.66 d_1^2 + 2.88 d_3 - 2.88 d_1 d_3 - 2.44 d_3^2)\mu^2 + (3.85 - 1.1764 d_1 - 4.9664 d_3)\mu + 0.2708 > 0$ for all $\mu > 0$, and it is in the black area if $p_1(\mu)p_2(\mu) - p_3(\mu) < 0$ for some $\mu > 0$. W-instability occurs on the boundary between these areas.

thresholds that are represented by the boundary between the white and black areas.

In these numerical simulations, the diffusion coefficients (d_1, d_3) are taken slightly inside the unstable (black) area in FIGURES 16, 17, 18, 19 and 20, and

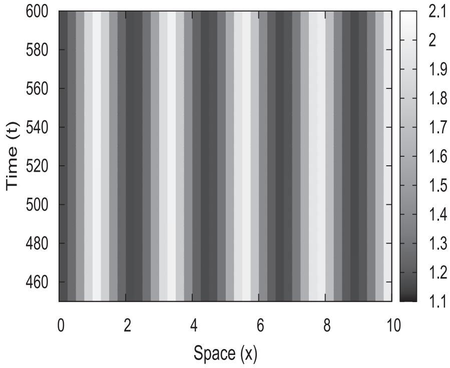

FIGURE 21

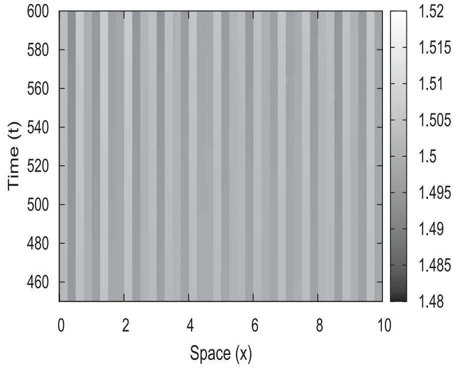

FIGURE 22

In FIGURE 21, we set $(p, q) = (1.5, 1.7)$, $(d_1, d_2, d_3) = (0.02, 0.96, 0.02)$, and in FIGURE 22, we set $(p, q) = (1.5, 2.7)$, $(d_1, d_2, d_3) = (0.004, 0.166, 0.83)$. Plotted in these figures are the numerical solutions $u(x, t)$ of (3.1), solved by semi-implicit schemes under the homogeneous Neumann boundary conditions.

the corresponding space-time profiles of $u(x, t)$ are shown. We used the semi-implicit scheme on the finite domain $((x, t) \in [0, 10] \times [0, 600])$, and the no flux boundary conditions are imposed on the boundary. For each simulation, the initial condition is a small sinusoidal perturbation of the homogeneous steady state. FIGURE 21 shows the steady bifurcation caused by the pair of type-2 unstable A_{13} and the stable A_2. FIGURE 22 shows the steady bifurcation caused by the pairs $(A_{13}\text{-}A_2)$ and $(A_1\text{-}A_{23})$.

FIGURE 23 exhibits the steady bifurcation caused by the pairs $(A_{13}\text{-}A_2)$ and $(A_1\text{-}A_{23})$, while FIGURE 24 is that caused by the pairs $(A_{13}\text{-}A_2)$ and $(A_1\text{-}A_{23})$.

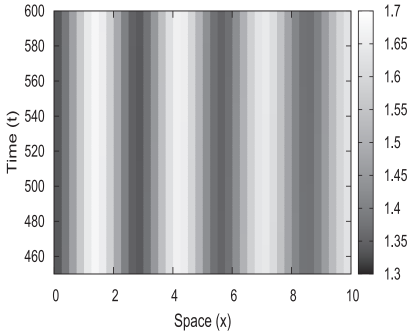

FIGURE 23

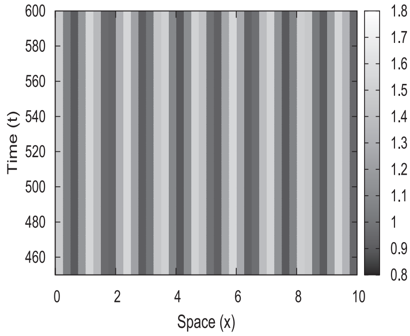

FIGURE 24

Parameter values are $(p, q) = (1.5, 3.5)$, $(d_1, d_2, d_3) = (0.1, 0.65, 0.25)$ in FIGURE 23, and $(p, q) = (1.2, 3.5)$, $(d_1, d_2, d_3) = (0.02, 0.15, 0.83)$ in FIGURE 24. The numerical solution $u(x, t)$ of (3.1) is plotted.

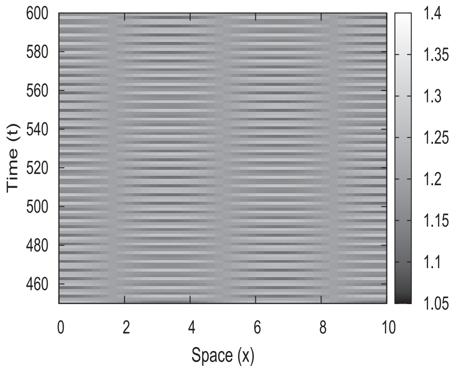

FIGURE 25. In FIGURE 25, we set $(p, q) = (1.2, 3.5)$, $(d_1, d_2, d_3) = (0.02, 0.09, 0.89)$, and the numerical solution $u(x, t)$ of (3.1), solved by semi-implicit schemes under the homogeneous Neumann boundary conditions, is plotted.

FIGURE 25 clearly exhibits the oscillatory Turing bifurcation caused by the pair (A_{12}-A_3). The W-wave number here is smaller than the S-wave number in FIGURE 24 above.

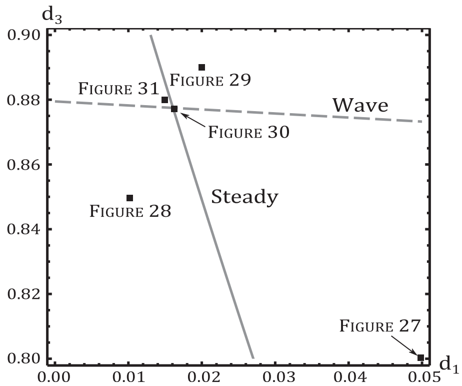

FIGURE 26. Parameters are set $(p, q) = (1.2, 3.5)$, and $d_2 = 1 - d_1 - d_3$.

In the left upper corner of FIGURES 19 and 20 with $(p, q) = (1.2, 3.5)$, we have shown that W-instability caused by type-1 unstable A_{12} and S-instability caused by the combined effects of type-3 unstable A_{13} and unstable subsystem A_1 interact at the linear level. FIGURE 26 is a magnification of the upper left corner near the double instability point where W-instability line (horizontal) and S-instability line (vertical) intersect at around $(d_1, d_3) = (0.0160811, 0.877466)$.

We now closely examine the interaction by numerically solving the nonlinear equation (3.1) for the diffusion rates d_1, d_2, d_3 near the double instability point where both S-instability and W-instability occur simultaneously. For the pairs of (d_1, d_3) indicated in FIGURE 26, we used the semi-implicit scheme to simulate the numerical solutions of (3.1) in the finite domain $(x, t) \in [0, 10] \times [0, 600]$ with the no flux boundary conditions. The gray scale profiles of $u(x, t)$ are shown as FIGURES 27 through to 31, below.

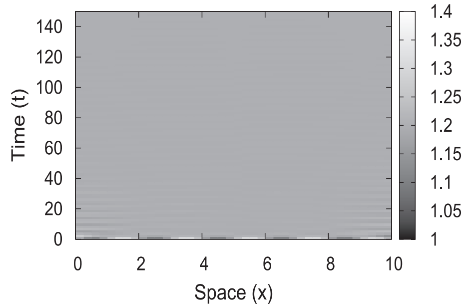

FIGURE 27. The parameter values in FIGURE 27 are given by

$$(p, q) = (1.2, 3.5), \quad (d_1, d_2, d_3) = (0.05, 0.15, 0.8),$$

and the numerical solution $u(x, t)$ of (3.1) is plotted.

This shows clearly that the steady state is stable.

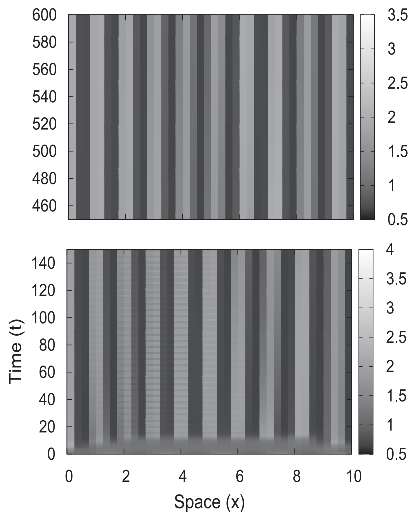

FIGURE 28

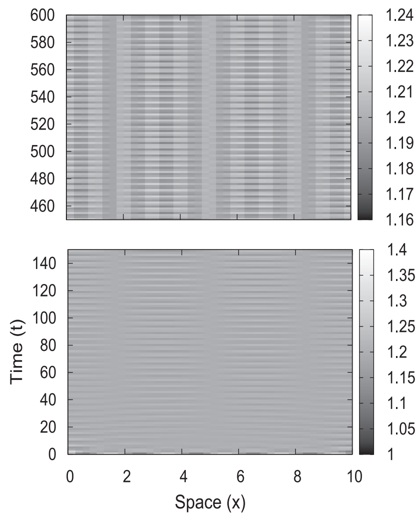

FIGURE 29

We set the parameters $(p, q) = (1.2, 3.5)$, $(d_1, d_2, d_3) = (0.01, 0.14, 0.85)$ in FIGURE 28, and $(p, q) = (1.2, 3.5)$, $(d_1, d_2, d_3) = (0.02, 0.09, 0.89)$ in FIGURE 29. The numerical solution $u(x, t)$ of (3.1) is plotted.

FIGURE 28, where we set $(d_1, d_2, d_3) = (0.01, 0.14, 0.85)$, shows S-instability with a slight influence of W-instability. FIGURE 29, which corresponds to $(d_1, d_2, d_3) = (0.02, 0.09, 0.89)$, clearly exhibits W-instability.

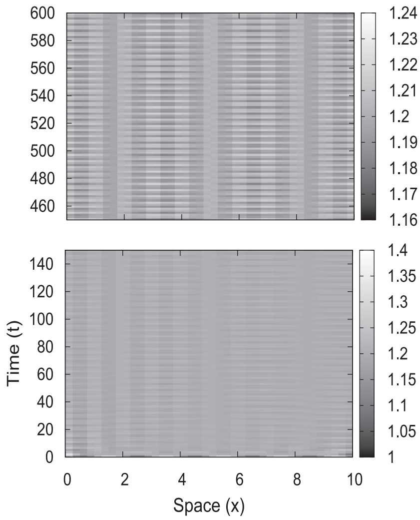

FIGURE 30

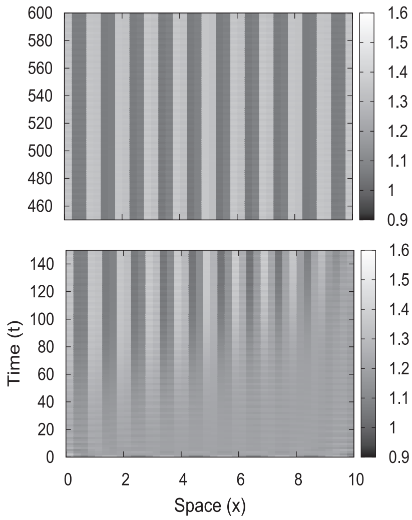

FIGURE 31

FIGURE 30: $(p, q) = (1.2, 3.5)$, $(d_1, d_2, d_3) = (0.0160811, 0.1064529, 0.877466)$. FIGURE 31: $(p, q) = (1.2, 3.5)$, $(d_1, d_2, d_3) = (0.015, 0.105, 0.88)$. We plotted the numerical solution $u(x, t)$ of (3.1) with the homogeneous Neumann boundary conditions solved by semi-implicit schemes.

By more detailed simulations, we have confirmed that bifurcations at these instabilities are supercritical. In FIGURE 30, where $(d_1, d_2, d_3) = (0.0160811, 0.1064529, 0.877466)$, the combined effect of S- and W-instability is visible. In FIGURE 31, where $(d_1, d_2, d_3) = (0.015, 0.105, 0.88)$ is employed, the dominant S-instability is superimposed by a weak W-instability. The bifurcation near the double point could be quite complicated, and we do not pursue its further study here.

4. Discussion

In this section, we classify stable 3×3 matrices to discern the range of applicability of our main results. We also point out several issues that are encountered when we deal with Turing instability in n-component systems ($n \geq 4$).

4.1. Classification of stable 3 × 3 matrices. In the previous section, we have exhibited a variety of unstable sub-matrices appearing in a stable 3×3 matrix A, and numerically investigated Turing instability associated with the unstable subsystems. A natural question arises: How many combinations of unstable subsystems are there within a stable 3×3 matrix A? The constraints are the stability conditions for A:

$$p_1 = -(\det A_1 + \det A_2 + \det A_3) > 0, \tag{4.1}$$

$$p_2 = \det A_{12} + \det A_{13} + \det A_{23} > 0, \tag{4.2}$$

$$p_3 = -\det A > 0, \quad p_1 p_2 - p_3 > 0. \tag{4.3}$$

We denote by $-$ (resp. $+$, 0) a stable (resp. unstable, neutral) 1-component subsystem of A. There are ten possible combinations of 1-component subsystems, and the constraint (4.1) gives immediately that the combinations $(+\,+\,+)$, $(+\,+\,0)$, $(+00)$, (000) do not appear in a stable matrix. On the other hand, by way of examples, we easily find that the following six types are possible for a stable A.

$$(-\,-\,-), \quad (-\,-\,+), \quad (-\,-\,0), \quad (-\,+\,+), \quad (-\,+\,0), \quad (-00).$$

We denote by T_0 (resp. T_1, T_2, T_3) a stable (resp. type-1 unstable, type-2 unstable, type-3 unstable) 2-component subsystem of A. There are twenty possible combinations of 2-component subsystems, and the following types do not appear in a stable A:

$$(T_1T_1T_1), \quad (T_1T_1T_3), \quad (T_1T_3T_3), \tag{4.4}$$

$$(T_2T_2T_2), \quad (T_2T_2T_3), \quad (T_2T_3T_3), \quad (T_3T_3T_3). \tag{4.5}$$

The combinations in (4.4) violate (4.1), while those in (4.5) violate (4.2). On the other hand, the remaining thirteen combinations in (4.6) below can constitute a stable matrix. Therefore, as long as the constraints (4.1) and (4.2) are satisfied, any combination of 2-component subsystems in (4.6) is realized in a stable 3×3 matrix.

$$\begin{array}{llll} (1)\ (T_0T_0T_0), & (2)\ (T_0T_0T_1), & (3)\ (T_0T_0T_2), & (4)\ (T_0T_0T_3), \\ (5)\ (T_0T_1T_1), & (6)\ (T_0T_1T_2), & (7)\ (T_0T_1T_3), & \\ (8)\ (T_0T_2T_2), & (9)\ (T_0T_2T_3), & (10)\ (T_0T_3T_3), & \\ (11)\ (T_1T_1T_2), & (12)\ (T_1T_2T_2), & (13)\ (T_1T_2T_3). & \end{array} \tag{4.6}$$

We have exhibited examples for (1), (2), (3) and (4) in the previous section. For completeness, we list examples for the other combinations.

$$(5)\ \begin{pmatrix} -2 & 1/4 & -1 \\ 0 & -2 & 7 \\ 7 & -1 & 3 \end{pmatrix}, \quad (6)\ \begin{pmatrix} 2 & -2 & 2 \\ 1.5 & -1 & -1 \\ -1 & 1 & -2.5 \end{pmatrix}, \quad (7)\ \begin{pmatrix} 2 & -2 & 2 \\ 1.5 & -1 & -1 \\ -1 & 1 & -1.5 \end{pmatrix},$$

$$(8)\ \begin{pmatrix} 1 & 1 & -4 \\ 2 & -2 & -2 \\ 2 & -2 & -1.5 \end{pmatrix}, \quad (9)\ \begin{pmatrix} 1 & 1.2 & 2 \\ 1 & 1 & 0 \\ -6.5 & -7 & -3 \end{pmatrix}, \quad (10)\ \begin{pmatrix} -2 & 0.55 & -2 \\ 0 & -2 & 5 \\ 2 & -1 & 3 \end{pmatrix},$$

$$(11)\ \begin{pmatrix} -2 & 1 & -4 \\ 5 & -2 & 15 \\ 4 & -3 & 3 \end{pmatrix}, \quad (12)\ \begin{pmatrix} 1 & -1 & 2 \\ 3 & -4 & 8 \\ -3 & 0 & 1 \end{pmatrix}, \quad (13)\ \begin{pmatrix} -2 & 1 & -4 \\ 5 & -2 & 0 \\ 4 & -1.7 & 3 \end{pmatrix}.$$

Among the combinations in (4.6), the last three (11), (12) and (13) seem most interesting, because the number of 2-component unstable subsystems is the maximum. We take (12) and show below how S- or W-instability appears as the diffusion rates d_1, d_2 and d_3 are varied. The matrix A in (12) is stable, and complementary pairs of subsystems are:

- $A_{12} = \begin{pmatrix} 1 & -1 \\ 3 & -4 \end{pmatrix}$: type-2 unstable, $A_3 = 1$: Unstable
- $A_{13} = \begin{pmatrix} 1 & 2 \\ -3 & 1 \end{pmatrix}$: type-1 unstable, $A_2 = -4$: Stable
- $A_{23} = \begin{pmatrix} -4 & 8 \\ 0 & 1 \end{pmatrix}$: type-2 unstable, $A_1 = 1$: Unstable

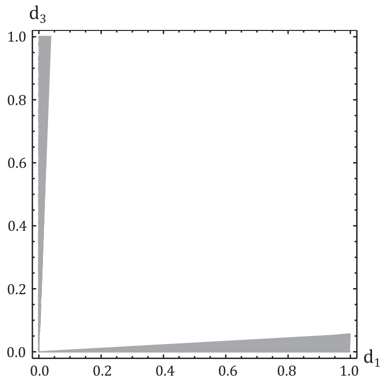

FIGURE 32

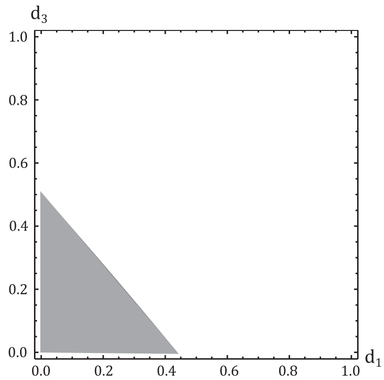

FIGURE 33

In FIGURE 32, $p_3(\mu) = d_1 d_3 \mu^3 + (-d_1 - d_3 + 4d_1 d_3)\mu^2 + (7 - 4d_1 - d_3)\mu + 1 > 0$ for all $\mu > 0$ in the while area. $p_3(\mu) < 0$ for some $\mu > 0$ in the gray area.
In FIGURE 33, $p_1(\mu)p_2(\mu) - p_3(\mu) = \{d_1 + d_3 + 2d_1 d_3 + (1 + d_1)d_3^2 + d_1^2(1 + d_3)\}\mu^3 + \{-2 + 3d_1^2 + 3d_3^2 + 4(d_1 + d_3 + d_1 d_3)\}\mu^2 + (-9 + 12d_1 + 9d_3)\mu + 3 > 0$ for all $\mu > 0$ in the while area. $p_1(\mu)p_2(\mu) - p_3(\mu) < 0$ for some $\mu > 0$ in the gray area.

In FIGURES 32 and 33, we set $d_2 = 1$. Two critical curves (the boundaries between white and gray areas) in FIGURE 32 show, respectively, the S-instabilities associated to $A_1 > 0$ with $d_1 \ll \min\{d_2, d_3\}$ and $A_3 > 0$ with $d_3 \ll \min\{d_1, d_2\}$. Theorem 1.2 (v) (together with its proof) predicts that S-instability does not occur for $(3 - \sqrt{8})d_1 < d_3 < (3 + \sqrt{8})d_1$, while a rough estimates read off from FIGURE 32 says that S-instability does not occur for $0.08d_1 < d_3 < 12.5d_1$. Note that $3 - \sqrt{8} \approx 0.17157$, $3 + \sqrt{8} \approx 5.82842$, and hence the theoretical results substantially underestimates the area where S-instability does not occur. The critical curve in FIGURE 33 indicates the location where W-instability associated to type-1 unstable A_{13} with $\max\{d_1, d_3\} \ll d_2$. On the part of this critical curve between the lines $d_3 = 0.08d_1$ and $d_3 = 12.5d_1$, the W-instability actually occurs primarily.

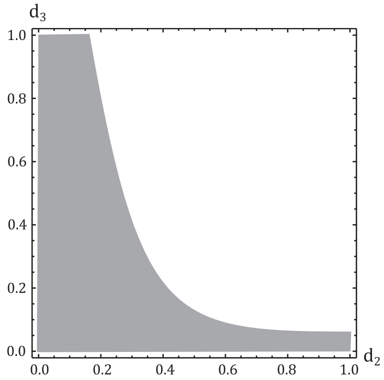

FIGURE 34

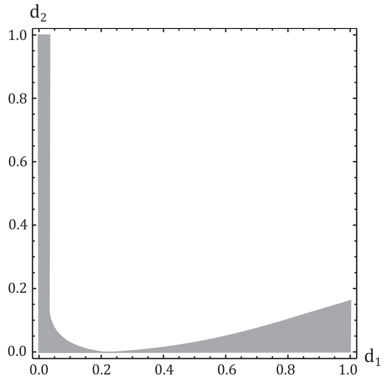

FIGURE 35

In FIGURE 34, $p_3(\mu) = d_2 d_3 \mu^3 + (-d_2 + 4d_3 - d_2 d_3)\mu^2 + (-7 + 4d_2 - d_3)\mu + 1 > 0$ for all $\mu > 0$ in the while area and $p_3(\mu) < 0$ for some $\mu > 0$ in the gray area, where $d_1 = 1$.
In FIGURE 35, $p_3(\mu) = d_1 d_2 \mu^3 + (4d_1 - d_2 - d_1 d_2)\mu^2 + (-1 - 4d_1 + 7d_2)\mu + 1 > 0$ for all $\mu > 0$ in the while area and $p_3(\mu) < 0$ for some $\mu > 0$ in the gray area, where $d_3 = 1$.

The critical curve in FIGURE 34 (FIGURE 35) indicates S-instability associated to type-2 unstable A_{23} (A_{12}).

4.2. Perspective for n-component systems. Let us consider (1.3) for n-component systems, where D is an $n \times n$ diagonal diffusion matrix and A is a stable $n \times n$ reaction matrix. Based on the discussion on 3-component systems, we present a probable mechanism of Turing instability in general n-component systems of reaction-diffusion equations.

Let I be a non empty subset of $\{1, 2, \ldots, n\}$. By A_I we denote the principal subsystem of A. Namely, A_I is the $m \times m$ submatrix obtained from A by taking exactly the rows and the columns of indices belonging to I, where m stands for the number of elements in I. For two subsets $I, J \subset \{1, 2, \ldots, n\}$ of indices, subsystems A_I and A_J are said to *form a complementary pair*, if $I \cap J = \emptyset$ and $I \cup J = \{1, 2, \ldots, n\}$ are satisfied. Then, a possible mechanism of Turing instability in n-component systems may be stated as follows.

(PM): *Suppose that A is a stable $n \times n$ matrix. If subsystems A_I and A_J of A form a complementary pair and A_I is unstable, then Turing instability occurs for diffusion matrices $D = \mathrm{diag}(d_1, d_2, \ldots, d_n)$ that satisfy*

$$\max_{k \in I}\{d_k\} \ll \min_{l \in J}\{d_l\}.$$

There are several issues to be considered before we prove or disprove this statement.

(A) What is the factor to detect W-instability? (The factor to detect S-instability apparently is $\det(-\mu D + A)$.)

(B) What type of Turing instability, S- or W-type, is associated to a type of unstable $m \times m$ subsystem A_I?
(C) What types of instabilities are there for $m \times m$ principal subsystems with $1 \le m < n$?
(D) When an unstable subsystem A_I is given, how does it form a stable matrix together with a suitable complementary partner?

Items (A) and (B) are related to the Routh-Hurwitz criteria for the stability of matrices. Items (C) and (D) are essentially classification problems of stable and unstable matrices. Let us clarify the points by considering 4×4 matrix A. We denote by $\lambda^4 + q_1\lambda^3 + q_2\lambda^2 + q_3\lambda + q_4$ the characteristic polynomial of A. Then, the stability conditions of A are

$$\text{(i)}\ q_1 > 0, \quad \text{(ii)}\ q_1q_2 - q_3 > 0, \quad \text{(iii)}\ q_1q_2q_3 - q_1^2q_4 - q_3^2 > 0, \quad \text{(iv)}\ q_4 > 0.$$

These conditions imply $q_3 > 0$ and $q_2 > 0$.

It is not difficult to show that A has a pair of pure imaginary roots ($\neq 0$) if the inequality in (iii) is replaced by equality. Applying this to the characteristic equation of $-\mu D + A$, we find W-instability is detected by examining how the polynomial

$$q_1(\mu)q_2(\mu)q_3(\mu) - q_1(\mu)^2q_4(\mu) - q_3(\mu)^2$$

in μ changes its sign for $\mu > 0$. Therefore, the question in item (A) is partially resolved for $n = 4$. However, it is cumbersome to extend this type of arguments to the general case $n \ge 5$.

A 4×4 matrix admits 1-, 2- and 3-component subsystems. We classified types of instability for 1- and 2-component subsystems. For a 3-component subsystem, let $\lambda^3 + p_1\lambda^2 + p_2\lambda + p_3$ be its characteristic polynomial. Types of its instability may be classified by negating the Routh-Hurwitz criteria (2.1), which leads us to at least 6 types. This seems to be intractable. The classification due to Tyson [17], given by negating qualitative stability conditions, may be one way. However, his method also becomes complicated as the size of the system exceeds 4.

Despite of these difficulties, the statement (PM) seems to be highly probable, and we may have to come up with a completely new idea to deal with Turing instability for general n-component systems.

Acknowledgement. The authors are grateful to Professor T. Ogawa and Professor Y. Morita for discussion and encouragement. The second author thank Professor S.-B. Hsu for his hospitality at NCTS of National Tsing Hua University where a preliminary version of this article was presented, polished and improved. We also thank the referee for helpful comments.

References

[1] M. Cross and H. Greenside, Pattern formation and dynamics in nonequilibrium systems, Cambridge University Press, Cambridge, UK, 2009.

[2] M. C. Cross and P. C. Hohenberg, Pattern formation outside of equilibrium, Rev. Mod. Phys. **65** (1993), 851–1112.
[3] F. R. Gantmacher, Applications of the theory of matrices, Inter-science Publishers Inc., NY, 1959.
[4] R. B. Hoyle, Pattern formation, An intorduction to methods, Cambridge University Press, Cambridge, UK, 2006.
[5] M. Mincheva and M. R. Roussel, A graph-theoretic method for detecting potential Turing bifurcations, J. Chem. Phys. **125**, 204102 (2006).
[6] J. D. Murray, Mathematical biology, Biomathematics texts, Springer-Verlag Berlin Heidelberg, 1989.
[7] A. Nakamasu, G. Takahashi, A. Kanbe and S. Kondo, Interactions between zebrafish pigment cells responsible for the generation of Turing patterns, Proc. Nat. Acad. Sci. **106** (2009), 8429–8434.
[8] T. Ogawa, Nonlinear phenomena and differential equations – bifurcation analyses of pattern dynamics – (in Japanese), Science-Sha, Tokyo, 2010.
[9] H. G. Othmer and L. E. Scriven, Interactions of reaction and diffusion in open systems, Ind. Eng. Chem. Fundamentals **8** (1969), 302–313.
[10] L. M. Pismen, Patterns and interfaces in dissipative dynamics, Springer-Verlag Berlin Heidelberg, 2006.
[11] A. B. Rovinsky and M. Menzinger, Chemical instability induced by a differential flow, Phys. Rev. Lett. **69** (1992), 1193–1196.
[12] A. M. Rovinsky and M. Menzinger, Differential flow instability in dynamical systems without an unstable (activator) subsystem, Phys. Rev. Lett. **72** (1994), 1193–1196.
[13] R. A. Satnoianu, M. Menzinger and P. K. Maini, Turing instabilities in general systems, J. Math. Biol. **41** (2000), 493–512.
[14] R. A. Satnoianu and P. van den Driessche, Some remarks on matrix stability with application to Turing instability, Linear Algebra and its Applications **398** (2005), 69–74.
[15] L. Szili and J. Tóth, Necessary condition of the Turing instability, Phys. Rev. E **48** (1993), 183–186.
[16] A. M. Turing, The chemical basis for morphogenesis, Phil. Trans. R. Soc. London, **B 273** (1952), 37–72.
[17] J. J. Tyson, Classification of instabilities in chemical reaction systems, J. Chem. Phys. **62** (1975), 1010–1015.
[18] K. A. J. White and C. A. Gilligan, Spatial heterogeneity in 3-species, plant-parasite-hyperparasite, systems. Phil. Trans. R. Soc. Lond. **B 353** (1998), 543–557.
[19] L. Yang, M. Dolnik, A. M. Zhabotinsky and I. R. Epstein, Pattern formation arising from interactions between Turing and wave instabilities, J. Chem. Phys. **117** (2002), 7259–7265.

Atsushi Anma
Department of Mathematical and Life Sciences
1-3-1 Kagamiyama, Higashi-Hiroshima
Hiroshima, 739-8526
Japan
E-mail: d100451@hiroshima-u.ac.jp

Kunimochi Sakamoto
Department of Mathematical and Life Sciences
1-3-1 Kagamiyama, Higashi-Hiroshima
Hiroshima, 739-8526
Japan
E-mail: kuni@math.sci.hiroshima-u.ac.jp

Tohru Yoneda
Fukuyama Meioudai High School
3-4-1 Meioudai, Fukuyama
Hiroshima, 720-0834
Japan
E-mail: t-yonedak882824@hiroshima-c.ed.jp